Appendix 3

How well can radiance reflected from the ocean-atmosphere system be predicted from measurements at the sea surface?

by

Howard R. Gordon and Tianming Zhang

Department of Physics
University of Miami
Coral Gables, FL 33124

(Accepted for publication in *Applied Optics*)

Abstract

There is interest in predicting the top-of-atmosphere (TOA) reflectance of the ocean-atmosphere system for in-orbit calibration of ocean color sensors. Here, using simulations, we examine the accuracy one could expect in estimating the reflectance ρ_T of the ocean-atmosphere system based on a measurement suite carried out at the sea surface, i.e., measurement of the normalized sky radiance (ρ_B) and the aerosol optical thickness (τ_a), under ideal conditions — a cloud free, horizontally-homogeneous atmosphere. Briefly, ρ_B and τ_a are inserted into a multiple-scattering inversion algorithm to retrieve the aerosol optical properties — the single scattering albedo and the scattering phase function. These retrieved quantities are then inserted into the radiative transfer equation to predict ρ_T. Most of the simulations were carried out in the near infrared (865 nm), where a larger fraction of ρ_T is contributed by aerosol scattering compared to molecular scattering, than in the visible, and where the water-leaving radiance can be neglected. The simulations suggest that ρ_T can be predicted with an uncertainty typically $\lesssim 1\%$ when the ρ_B and τ_a measurements are error free. The influence of the simplifying assumptions that were made in the inversion-prediction process, such as, modeling the atmosphere as a plane-parallel medium, employing a smooth sea surface in the inversion algorithm, using scalar radiative transfer theory, and assuming that the aerosol was confined to a thin layer just above the sea surface, was investigated. In most cases, these assumptions did not increase the error beyond $\pm 1\%$. An exception was the use of scalar radiative transfer theory, for which the error grew to as much as $\sim 2.5\%$, suggesting that using ρ_B-inversion and ρ_T-prediction codes that include polarization would be more appropriate. However, their use would necessitate measurement of the polarization associated with ρ_B. The uncertainty introduced by unknown aerosol vertical structure was also investigated and found to be negligible if the aerosols were nonabsorbing or weakly absorbing. Extension of the analysis to the blue, which requires measurement of the water-leaving radiance, showed significantly better predictions of ρ_T because the major portion of ρ_T is the result of molecular scattering, which is precisely known. We also simulated the influence of calibration errors in both the sun photometer and ρ_B radiometer. The results suggest that the relative error in the predicted ρ_T is similar in magnitude to that in ρ_B (actually it was somewhat less). However, the relative error in ρ_T induced by error in τ_a is usually $\ll$ the relative error in τ_a. Presently, it appears that radiometers can be calibrated with an

uncertainty of $\sim \pm 2.5\%$, therefore it is reasonable to conclude that, at present, the most important error source in the prediction of ρ_T from ρ_B is likely to be error in the ρ_B measurement.

1. Introduction

Most satellite remote sensing instruments show significant variations in radiometric sensitivity after launch. Because of this, considerable effort has been placed on so-called *vicarious* calibration, i.e., in-orbit calibration utilizing the radiance predicted at the sensor by a variety of methods.[1–12] Some sensors, e.g., the Polarization and Directionality of Earth Radiation[13] (POLDER) to be launched on the Advanced Earth Observation Satellite (ADEOS), have no on-board provision for examination of the radiometric performance, so the entire calibration strategy must be a vicarious effort.

The prediction of the radiance at the sensor can be made by using high-altitude aircraft radiometric measurements extrapolated to the top-of-the-atmosphere (TOA).[7,9] Alternatively, one can make measurements of the surface reflectance and the aerosol optical thickness from the ground, followed by scattering computations to estimate the aerosol scattering phase function and the single scattering albedo, e.g., using Mie theory, and radiative transfer computations to predict the TOA radiance.[9] The focus of this paper is the accuracy with which the TOA radiance can be predicted by the latter method under ideal circumstances — a cloud-free horizontally-homogeneous atmosphere. However, as we wish to remove as many assumptions as possible regarding the aerosol, we derive estimates of the aerosol scattering phase function and single scattering albedo using sky radiance measurements, rather than computing them using Mie theory. In this way, questions regarding the error in the estimate of these radiatively important parameters due to errors in the estimated aerosol complex index of refraction and the size (and shape) distribution are circumvented. Since our interest is mainly in sensors for measuring the color of the ocean, e.g., the Sea-Viewing Wide-field-of-view Sensor[14] (SeaWiFS) and the Moderate Resolution Spectral Radiometer[15] (MODIS), we restrict our analysis to situations when sensors are viewing the oceans as opposed to the land surface. The analysis is still valid for calibrating sensors designed for the land surface when they are over the oceans, but in practice that would only be useful for vicarious calibration of the low end of their radiometric sensitivity.

We assume the following measurements, carried out at the sea surface, are available for the analysis: (1) the aerosol optical thickness at the wavelength of interest measured by a radiometer

with a narrow field of view aimed directly at the sun (sun photometer); and (2) the sky radiance at the wavelength of interest measured in the solar almucantar and in the principal plane. Since a large portion of the TOA radiance over the oceans is due to backscattering from the aerosol, we will assume that the solar zenith angle is sufficiently large that such backscattering can be assessed with the surface measurements, e.g., solar zenith angles $\gtrsim 60°$. Using these measurements (simulated by solving the radiative transfer equation), we apply a variant of the inversion algorithm developed by Wang and Gordon[16] to retrieve the columnar aerosol scattering phase function and the single scattering albedo. These retrieved optical properties are then inserted into the radiative transfer equation to predict the TOA radiance for comparison with that based on the true optical properties of the atmosphere, and to determinate the error in the procedure. Then, we examine the influence of errors in the measurement of the sky radiance and the aerosol optical thickness. Next, we examine the possible reduction of accuracy when measurements of the solar aureole (which is difficult to measure from a ship) are absent. Finally, we examine the effects of the assumptions used in the retrieval-prediction process, e.g., the use of scalar radiative transfer theory for a plane parallel atmosphere over a smooth sea surface.

2. Basis of estimation of TOA radiance

The basic idea for the estimation of the radiance, $L_T(\theta_T)$, at the TOA given the aerosol optical thickness, τ_a, and radiance measurements, $L_B(\theta_B)$, at the bottom of the atmosphere (BOA), is provided schematically in Figure 1. We normalize the radiances, L's, to form normalized radiances (or generalized reflectances and transmittances), ρ's, given by $\rho = \pi L / F_0 \cos\theta_0$, where F_0 is the extraterrestrial solar irradiance and θ_0 is the solar zenith angle. If we ignore the presence of the ocean, i.e, we assume it is totally absorbing, ignore molecular (Rayleigh) scattering, and assume that τ_a is sufficiently small that the single scattering approximation is appropriate, then, for the geometry shown in the figure, the normalized radiances are given by

$$\begin{aligned} \rho_T(\theta_T) &= \frac{\omega_0 P(\Theta)\tau_a}{4\cos\theta_T \cos\theta_0}, \\ \rho_B(\theta_B) &= \frac{\omega_0 P(\Theta)\tau_a}{4\cos\theta_B \cos\theta_0}, \end{aligned} \tag{1}$$

where ω_0 is the single scattering albedo of the aerosol, $P(\Theta)$ is the aerosol scattering phase function, and Θ is the scattering angle common to both viewing directions (Figure 1). Thus, in the geometry shown,

$$\cos\theta_T \rho_T(\theta_T) = \cos\theta_B \rho_B(\theta_B), \tag{2}$$

and the radiance $L_T(\theta_T)$ is completely determined from the radiance $L_B(\theta_B)$. Alternatively, one could use Eq. (1) to estimate the value of $\omega_0 P(\Theta)\tau_a$ for all values of Θ available from the surface, and then evaluate L_T for those directions for which $\omega_0 P(\Theta)\tau_a$ is available. Note that to compute L_T from L_B, independent measurement of the aerosol optical thickness is not required. If Rayleigh scattering is also present, then $\omega_0 P(\Theta)\tau_a$ in Eq. (1) must be replaced by $\omega_0 P(\Theta)\tau_a + P_r(\Theta)\tau_r$, where $P_r(\Theta)$ is the Rayleigh scattering phase function and τ_r is the Rayleigh optical thickness; however, it is still possible to compute L_T from L_B without an independent measurement of the aerosol optical thickness.

In this simple example, we see that in the limit of small optical thickness, the only error in the radiance L_T is the measurement error in L_B. In fact, Eq. (2) shows that the fractional errors in L_T, L_B, ρ_T, and ρ_B are all identical — the radiative transfer process introduces no additional error in L_T or ρ_T. This is an important conclusion that we shall see is approximately true, even in a multiple-scattering atmosphere bounded by a Fresnel-reflecting sea surface, i.e., the error added by the radiative transfer process is small.

3. Estimation of the aerosol optical properties.

In the presence of a Fresnel-reflecting sea surface, the situation is more complex because of reflection from the surface. For example, at the TOA, reflection of the solar beam from the surface followed by scattering, or reflection from the sea surface of radiance scattered from the incident solar beam, can make a significant contribution to ρ_T. Similarly, scattering from the surface-reflected solar beam contributes to ρ_B. This is true even in the single-scattering regime, where it is easy to see that there is no geometry in which a simple analytical expression similar to Eq. (2) exists. In this case it is necessary to employ a two-step procedure to estimate ρ_T from ρ_B. In the first step, one retrieves $\omega_0 P(\Theta)\tau_a$ from the measurement of $\rho_B(\theta)$, and in the second step, this quantity

is used to predict $\rho_T(\theta)$. In this section we discuss the first step, retrieval of the aerosol optical properties.

3.A. Limit of small optical depth

In the absence of Rayleigh scattering and in the presence of a Fresnel-reflecting sea surface, the relationship between $\rho_B(\theta_B)$ and the aerosol properties is

$$\rho_B(\theta_B) = \frac{\omega_0 \tau_a}{4 \cos\theta_B \cos\theta_0} \Big[P(\Theta) + r(\theta_0) P(\Theta_B^r) \Big], \tag{3}$$

where $r(\alpha)$ is the Fresnel reflectance of the flat sea surface for an incident angle α. The first term in the square brackets represents the contribution from photons scattered through an angle Θ by the incident solar beam *before* it reflects from the sea surface, while the second term represents the contribution from photons scattered through an angle Θ_B^r by the incident solar beam *after* it has reflected from the surface. For most aerosol phase functions, the second term will be negligible for values of θ_B for which $\Theta \lesssim 50°$; however, for larger values of Θ, the second term can make a significant contribution ($\sim 30\%$) to $\rho_B(\theta_B)$, and interferes with the estimation of $P(\Theta)$. In fact, there is no set of measurements that can be used to uniquely separate the two terms in Eq. (3), and provide $\omega_0 P(\Theta)\tau_a$. Thus, in contrast to the situation with the sea surface absent, for which $\omega_0 P(\Theta)\tau_a$ could be precisely estimated for $\Theta < \pi/2 + \theta_0$ using Eq. (1), when the sea surface is present this is not possible.

We now examine how one might extract $\omega_0 P(\Theta)\tau_a$ from measurements of ρ_B. We consider two schemes for effecting this: (1) using ρ_B measured in the principal plane (PP), and (2) combining principal plane and solar almucantar measurements (PP+A). The largest scattering angle accessible to direct observation (the first term in Eq. (3)) is $\Theta_{\mathbf{Max}} = \pi/2 + \theta_0$. It is unrealistic to expect to retrieve accurate values of $\omega_0 P(\Theta)\tau_a$ for larger scattering angles, because their contribution to ρ_B always involves $r(\theta_0)$, which in a typical experiment ($\theta_0 \sim 60°$) will be < 0.1. For larger values of θ_0, $r(\theta_0)$ will be even larger which further increases the difficulty. Thus, some assumption regarding $P(\Theta)$ for $\Theta > \pi/2 + \theta_0$ is necessary. The assumption that we use is that $P(\Theta) = P(\Theta_{\mathbf{Max}})$ for $\Theta > \Theta_{\mathbf{Max}}$. [Actually we assume that this is true for Θ a few degrees $< \Theta_{\mathbf{Max}}$ because measurements

cannot be made at the horizon.] With this assumption, $\rho_B(\theta_B)$ measured in the principal plane with $\theta_B \sim 90°$ in a direction opposite to the sun (viewing in a direction with the sun at the observer's back) can be used to provide $\omega_0 P(\Theta)\tau_a$ for $\Theta > \Theta_{\mathbf{Max}}$. Measurements of $\rho_B(\theta_B)$ in the rest of the principal plane can then be used to provide $\omega_0 P(\Theta)\tau_a$ for $\Theta < \Theta_{\mathbf{Max}}$. An alternative scheme which provides more accurate values of $\omega_0 P(\Theta)\tau_a$ near $\Theta = 90°$ is to use values of $\rho_B(\theta_B)$ in the principal plane (opposite to the sun) for only $\theta_0 \leq \theta_B \leq 90°$ to obtain $\omega_0 P(\Theta)\tau_a$ for $\Theta > 2\theta_0$, and then use the almucantar values to obtain it for $\Theta < 2\theta_0$. In the second procedure, the dependence of ρ_B on the estimated part of the phase function ($\Theta > \Theta_{\mathbf{Max}}$) is quadratic in τ, rather than linear, for $\Theta <$ some angle Θ'. This reduces the error in $\omega_0 P(\Theta)\tau_a$ for $\Theta < \Theta'$. In the case we concentrate on in detail in this paper, $\theta_0 = 60°$, $\Theta' \approx 110°$.

We tested these ideas by assuming that single scattering was the correct physics and computing ρ_t at 865 nm using the Maritime aerosol model of Shettle and Fenn[17] with a relative humidity of 99%, which we indicate by M99. The scattering phase function for M99 computed from Mie theory is provided in Figure 2. The M99 model is employed because it yields the most sharply peaked phase function with the most structure in the vicinity of the rainbow angle ($\Theta \sim 140°$), of any of the Shettle and Fenn models. These characteristics make accurate retrieval of $\omega_0 P(\Theta)\tau_a$ particularly difficult, and as such, provide a severe test of the technique. Figure 3 provides the error in the retrieved values of $\omega_0 P(\Theta)\tau_a$ obtained for $\theta_0 = 60°$ using these two methods for the M99 aerosol model. The large error for $\Theta > 150°$ is expected, as this is the region for which a guess was made for $\omega_0 P(\Theta)\tau_a$. The large spike near $\Theta = 120°$ results from the large error in the estimated $\omega_0 P(\Theta)\tau_a$ near the backscattering direction. The small spike near $\Theta = 90°$ for the PP+A case is due to the overestimation of $\omega_0 P(\Theta)\tau_a$ near $\Theta = 120°$. In the forward direction, the error is negligible. Clearly, the PP+A method is superior to the PP method. It should be noted that if the aerosol had a phase function with less backscattering (and/or less variation in backscattering with Θ), the error would be significantly reduced. For example, using the Shettle and Fenn Tropospheric model at 50% relative humidity (T50 in Figure 2) under the same conditions, resulted in a maximum error for $\Theta < \Theta_{\mathbf{Max}}$ of $\sim$1.9%.

3.B. The multiple scattering regime

In general, the single-scattering approximation will not be valid, and its application will result in very poor retrievals. We carried out multiple scattering computations using the same aerosol model as in the example above (M99 at 865 nm) with an aerosol optical thickness of 0.2 to simulate ρ_T and ρ_B. After subtraction of the component due to molecular scattering, the single scattering formula Eq. (3) was used to derive $\omega_0 P(\Theta)$. The error in the retrieved $\omega_0 P(\Theta)$ was nearly a factor of two for $\Theta \gtrsim 80°$. Clearly, multiple scattering must be considered in carrying out such inversions.

A procedure similar to that in the single scattering case can be employed in a multiply scattering atmosphere, i.e., we will use the surface measurements to estimate ω_0 and $P(\Theta)$. The estimate of ω_0 and $P(\Theta)$ is effected by using the retrieval algorithm described by Wang and Gordon.[16] Based on measurement of the sky radiance and the aerosol optical thickness at the sea surface, the Wang and Gordon algorithm finds aerosol optical properties that, when inserted into the radiative transfer equation (RTE), yield the measured values of ρ_B. This is accomplished in the following manner. With initial guesses for ω_0 and $P(\Theta)$, the RTE is solved using the measured value of τ_a to find the predicted sky radiance. The differences $\Delta\rho(\hat{\xi}_B)$, where $-\hat{\xi}_B$ denotes the direction in which the radiometer points in the sky, between the predicted and measured sky radiance is then used to estimate a new phase function and value for ω_0. This estimate is accomplished using the single scattering approximation, Eq. (1), i.e., ignoring the Fresnel reflection contribution $r(\theta_0)$, in the following manner. First, the scattering angle Θ_B that would be appropriate to the single scattering of the direct incident solar radiation in the direction $\hat{\xi}_B$ is determined for each point at which the sky radiance is measured, i.e., each $\hat{\xi}_B$. Next, the error in the computed sky radiance is used to estimate the error $\Delta[\omega_0 P(\Theta_B)]$ in the trial value of $\omega_0 P(\Theta_B)$ using the single scattering formula. Finally, the value of $\omega_0 P(\Theta_B)$ is then changed by a fraction (usually 0.5) of $\Delta[\omega_0 P(\Theta_B)]$ yielding a revised value. The revised $\omega_0 P(\Theta_B)$ is then inserted into the RTE and new values of $\rho_t(\hat{\xi}_B)$ are computed. The process is repeated until the measured and computed $\rho_B(\hat{\xi}_B)$ are in agreement within the experimental error. Using pseudo data simulated by solving the RTE for a two-layer atmosphere (aerosols in the lower layer) bounded by a flat Fresnel-reflecting sea surface, Wang and Gordon[16] found that the rms error between the measured and computed $\rho_B(\hat{\xi}_B)$'s could usually be reduced to a fraction of 1% when the correct vertical structure was employed in the correction algorithm.

As in the single scattering case, there are scattering angles Θ that are inaccessible with this procedure, i.e., the maximum value of Θ is $\Theta_{\mathbf{Max}} = \pi/2 + \theta_0$, where θ_0 is the solar zenith angle. Thus, there is no way to derive $P(\Theta)$ for $\Theta > \Theta_{\mathbf{Max}}$. For these angles, a guess is made for P, e.g., $P(\Theta) = P(\Theta_{\mathbf{Max}})$ for $\Theta > \Theta_{\mathbf{Max}}$. The guess enables the completion of the phase function for the next iteration and also for the estimation of ω_0 from $\omega_0 P(\Theta)$ by integration over solid angle.

As an example of this procedure, we carried out multiple scattering computations of ρ_B at a wavelength of 865 nm. We used an aerosol optical thickness of 0.2 and assumed that the aerosol was all located in the marine boundary layer, i.e., a physically thin layer at the bottom of the atmosphere. For reference, this value for τ_a is about two to three times the average for the North Atlantic in a pure maritime atmosphere.[18] The error in the resulting retrieval is provided in Figure 4. The retrieved ω_0 (0.986) compares favorably with the true value of 0.998. The small bump in the retrieval near $\Theta = 120°$ is due to reflection of the solar beam from the sea surface and subsequent scattering through $\sim 180°$. It would not appear were $\omega_0 P(\Theta)$ estimated accurately near $\Theta = 180°$. It could be removed by simply not using the almucantar and principal plane pseudo data for scattering angles near $\Theta = 120°$, or its presence could be used to improve the estimate of $\omega_0 P(\Theta)$ near $\Theta = 180°$. As we have not thoroughly investigated its removal or use, we shall simply ignore its presence here, i.e., when we estimate the TOA radiance, we will know what viewing angles will be influenced by its presence and simply avoid those viewing angles. Clearly, the retrieval in this multiple-scattering atmosphere is nearly as effective as it would be were single scattering the correct physics (Figure 3).

It is important to note that this procedure provides a full multiple scattering inversion of the sky radiance; the single scattering formulas are *only* used to provide a coarse estimate of the amount that $\omega_0 P(\Theta)$ should be changed at each step of the iteration. As mentioned above, had we used the single-scattering algorithm of Section 3.A, the error in the retrieved $\omega_0 P(\Theta)$ for $80° \lesssim \Theta \lesssim 130°$ would have been $\sim$ a factor of two or greater.

4. Estimation of the TOA radiance

In this section we apply the retrieved aerosol properties to estimate the radiance exiting the TOA in the perpendicular plane, near where most ocean color instruments view.

4.A. Limit of small optical depth.

In the limit of small τ_a, the reflectance at the TOA is simply given by

$$\rho_T(\theta_T) = \frac{\omega_0 \tau_a}{4 \cos\theta_T \cos\theta_0} \Big[P(\Theta) + [r(\theta_T) + r(\theta_0)] P(\Theta_T^r) \Big], \tag{4}$$

where Θ_T^r is the appropriate angle for scattering the surface-reflected solar beam toward the sensor. We need only insert the retrieved $\omega_0 P(\Theta)\tau_a$ into this expression to predict ρ_T. Figure 5 provides the error in $\rho_T(\theta_T)$ using the single-scattering estimate of $\omega_0 P(\Theta)\tau_a$ derived in Section 3.C by the two methods. As expected, the PP+A method is superior to the PP method alone. When the PP+A method is used, the relative error in ρ_T (or L_T) is $\lesssim 2.5\%$ for $\theta_T \gtrsim 15°$. Note that we have ignored any molecular scattering component in ρ_T. As this component is precisely known, including it in the analysis will reduce the error in ρ_T in Figure 5 by a factor $(1 + \rho_M/\rho_A)$, where ρ_M and ρ_A are, respectively, the molecular and aerosol contributions to ρ_T.

4.B. The multiple-scattering regime.

Given the values of ω_0 and $P(\Theta)$, estimated from measurements of ρ_B and τ_a, prediction of the radiance at the TOA is straightforward. We simply insert $\omega_0 P(\Theta)$ and τ_a into the RTE with an assumed aerosol vertical profile and solve for the radiance. In this section we examine the accuracy of the TOA-radiance computed in this manner. As in the single scattering case, we examine the error induced by errors in τ_a and in $\rho_B(\theta_B)$.

As described in Section 3.B, we simulated the sky radiance and the associated TOA radiances using the M99 aerosol model with $\tau_a = 0.2$ at 865 nm in the lower layer of a two-layer atmosphere. All molecular scattering (Rayleigh scattering) was placed in the upper layer. The solar zenith angle at the time of the sky radiance measurement was taken to be 60°. The sky radiance was assumed to be measured in the solar almucantar (beginning with an azimuth angle 1° from the sun)

and from the zenith to near the horizon in the principal plane, facing away from the sun (PP+A measurements). Figure 4 provides the error in the retrieved ω_0 and $\omega_0 P(\Theta)$ for this case.

The retrieved $\omega_0 P(\Theta)$ and the measured value of τ_a were then inserted into the RTE and the resulting radiance at the TOA was computed. Figure 6 provides the error in the computed TOA radiance, i.e., the percent difference between the reflectance ρ_T computed using the retrieved aerosol optical properties and that computed using the true aerosol optical properties. At the TOA viewing was assumed to take place in the perpendicular plane, i.e., the azimuth of the viewing angle was taken normal to the plane formed by the sun's rays and the zenith. The TOA computations were carried out for solar zenith angles of 60°, 50°, and 45°, where for the latter two it was assumed that the aerosol is unchanged in concentration or properties as θ_0 varies from 60° to 45°. The reason for considering these other values of θ_0 was to simulate the measurement of the aerosol optical properties when θ_0 is large (so that $\omega_0 P(\Theta)$ can be obtained at large values of Θ), but computation of the TOA radiance when a satellite sensor might view the surface (later in the day, therefore a smaller value of θ_0). The retrieval of $\omega_0 P(\Theta)$ and the subsequent computation of ρ_T, for each solar zenith angle, was carried out for several values of τ_a in order to determine the effect of measurement error in τ_a on the TOA radiance. It is important to note that the same value of τ_a was used in the retrieval algorithm and the TOA-radiance prediction code during this process; however, the value of τ_a used to generate the pseudo data was 0.2. Error in the measurement of τ_a is manifest in error in the retrieved value of ω_0. Table 1 provides the retrieved value of ω_0 corresponding to a given value of τ_a.

The large spike in error in the TOA radiance for $\theta_0 = 50°$ and 45°, Figures 6c and 6d, respectively, is due to the bump in the retrieved phase function near $\Theta = 120°$. Ignoring this, the results presented in the figures clearly show that when the correct value of τ_a is avaliable the error in the predicted TOA radiance is always less than 2% and is usually $\lesssim$ 1% as long as $\theta_T \lesssim 60°$, a condition met by all satellite-borne scanning radiometers of interest. A given percent error in τ_a results in a significantly smaller percent error in the TOA radiance, e.g., a 30% error in τ_a produces at most a $\sim$ 3% error in radiance at $\theta_0 = 60°$, a 5% error at $\theta_0 = 50°$, and $\lesssim$ 9% error at $\theta_0 = 45°$.

This is consistent with the fact that τ_a is not even required in the single scattering regime (Section 2).

Figure 7 provides the error in the predicted TOA radiance for a given error in the measured radiance at the surface. It was assumed that a single radiometer is used to measure L_B, and therefore the calibration error was taken to be the same for all the measurement angles (here $\pm 5\%$). In contrast to the small effect that error in τ_a has on the predicted TOA radiance, error in L_B results in an error of similar magnitude in the predicted L_T. This is also in agreement with the single scattering analysis in Section 2. Thus, the results of the simulations presented in this section suggest that the radiative transfer process in the multiple scattering regime does not add significant error to the prediction of L_T over and above that predicted by the single scattering analysis. As the optical thickness increases, the accuracy of the method will likely decrease, and the sensitivity to error will surely increase; however, the value of τ_a used here is already high for the marine atmosphere,[18–20] so the method should be applicable in most situations.

5. Sensitivity analysis.

In this section we report the sensitivity of the predicted TOA radiances to the various assumptions that were made in the retrieval process. In particular, we examine the effect of omitting measurement of the solar aureole, the effect of an incorrect assumption regarding the vertical structure of the atmosphere, and the effects of ignoring the roughness of the sea surface, the curvature of the atmosphere, and the polarization of the radiation, in the $\omega_0 P(\Theta)$ retrieval algorithm.

5.A. Absence of solar aureole measurements.

In the results presented in Section 4.B for multiple scattering it was assumed that measurements of the sky radiance could be made at angles as small as 0.92° from the sun. In practice, this is very difficult. However, Nakajima et al.,[21] have reported solar aureole measurements to angles as small as 2° from the sun. For measurements carried out at sea, the motion of the ship requires the use of an all-sky camera[22] for measuring the sky radiance and, due to dynamic range limitations,

a portion of the aureole must be blocked in such measurements. This further restricts the amount of the solar aureole that can be obtained. Thus, it is important to understand the effect that the minimum angle that can be observed in the solar aureole has on the prediction of the radiance at the top of the atmosphere, from ρ_B measured at the surface. The difficulty with not measuring a significant portion of the solar aureole is that in the inversion process there will be an inconsistency between the measured value of τ_a and the aerosol phase function at each stage of the iteration process. Because of the lack of small-angle measurements, the phase function will not be correct in the aureole region for aerosols possessing a phase function with a strong forward peak. For such aerosols, a significant portion of the aerosol optical thickness is due to small-angle scattering. Thus if the aureole is not measured, usually a smaller value of τ_a would be appropriate in the inversion process to arrive at the correct values of $\omega_0 P(\Theta)$ outside the aureole region.

To investigate the aureole influence, we repeated the computations carried out in Section 4.B for three simulations in which pseudo data in the almucantar with $\Theta_{\text{Min}} = 2.62°$, 8.68°, and 17.33° were utilized. Figure 8 provides the error in the TOA radiance when $\Theta_{\text{Min}} = 2.62°$, a value that would be possible if the measurements were made from a stable platform such as an island. As before, in addition to the correct value of τ_a, the computations were also carried out for six other values of τ_a near the correct value. It is seen that the error in the TOA radiance is similar to that in Figure 7, where $\Theta_{\text{Min}} = 0.92°$. Figures 9 and 10 provide the error for $\Theta_{\text{Min}} = 8.68°$ and 17.33° respectively. Examination of these shows that when the measurements are made at $\theta_0 = 60°$ and the TOA-radiance is constructed at the same value of θ_0 the error is only slightly greater than that provided in Figure 7; however, when the TOA radiance is predicted at $\theta_0 = 45°$ and 50°, the inconsistency between the measured value of τ_a and the aerosol phase function is apparent. To achieve small errors in the TOA radiance a smaller value of τ_a must be used in both the retrieval and the TOA-radiance prediction codes. Is there any way of knowing what value of τ_a to use? Table 2 provides the values of ω_0 retrieved in our simulations for a given value of Θ_{Min} and τ_a. Comparing Figures 8–10 with Table 2, one sees that when the value of τ_a that produces a value of ω_0 that is closest to the correct value is used in these two codes, the error is essentially the same as the error for $\Theta_{\text{Min}} = 0.92°$. But how can we know the correct value of ω_0? In general there is no way of knowing ω_0; however, in an open-ocean regime in which the aerosol is locally

generated, it is reasonable to expect that ω_0 will be very close to unity. As aureole measurements need only be absent when the sky radiance is measured from a ship at sea, the assumption that $\omega_0 \approx 1$ should be justified when it is needed. An alternate method of dealing with the absence of aureole measurements is discussed in the appendix.

5.B. Incorrect vertical structure assumed in the inversion algorithm.

In all of the simulations studied in Section 4.B, the vertical structure of the atmosphere — two layers with all of the aerosols in the lower layer and all of the molecular scattering confined to the upper layer — assumed in the inversion code, and also the code to predict the TOA radiance from the retrieved optical properties, was the same as the vertical structure used to generate the pseudo data, i.e., the correct vertical structure was used in the retrieval and prediction process. As the aerosol over the oceans is usually mostly confined to the marine boundary layer, we expect this to be similar to the typical situation. However, it is important to understand the error in the TOA radiances when an incorrect vertical structure is assumed. For this purpose, we generated pseudo sky radiance data using the following vertical structure of the atmosphere: a maritime aerosol in the marine boundary layer (M99 in Figure 2) and an aerosol represented by the Shettle and Fenn[17] tropospheric model with a 50% relative humidity (T50 in Figure 2) in the free troposphere. The aerosol optical thickness were taken to be 0.15 and 0.05 in the boundary layer and free troposphere, respectively. The thickness of the boundary layer was assumed to be $\sim$ 2 km, so 22% of the molecular scattering was placed in the lower layer and 78% in the free troposphere. It was assumed that the total aerosol optical thickness was correctly measured, i.e., the measured τ_a was assumed to be error free. The pseudo data were introduced into the $\omega_0 P(\Theta)$ retrieval algorithm used in Section 4.B, which assumed a vertical structure in which all of the aerosol was in the boundary layer and the free troposphere was aerosol free. Thus, an incorrect vertical structure was assumed in the retrieval algorithm. The same incorrect vertical structure was also used in the TOA radiance-prediction code. Figure 11 provides the error in the predicted TOA radiance using this procedure. It is seen that the error is not significantly different from that shown in Figure 6, i.e., $\lesssim$ 1.5%. If the correct vertical structure were known, e.g., from LIDAR observations, and used in the retrieval and TOA-radiance prediction codes the resulting error is provided in Figure 12. In this case it

was assumed in the retrieval process that the aerosol possesses the same $\omega_0 P(\Theta)$ in both layers, but τ_a was correctly divided between the two layers. Comparison of Figures 11 and 12 shows that using the correct vertical structure leads to some improvement; however, it does not appear that significantly better results are obtained by knowing the vertical structure of the aerosol. These simulations suggest that knowledge of the vertical structure of the atmosphere is not critical for estimating the TOA radiance from measurements of ρ_B and τ_a.

The aerosol models used in the preparation of Figures 11 and 12 were only weakly absorbing, i.e., ω_0 was ≈ 0.930 and 0.999 for T50 and M99, respectively. To examine the effect of a strongly-absorbing aerosol, we replaced T50 in the simulations presented in Figures 11 and 12 with the Shettle and Fenn Urban model for a relative humidity of 50% (U50). For U50, $\omega_0 \approx 0.603$ at 865 nm. This situation could represent an example of a layer of polluted urban air transported over the ocean above the marine boundary layer. Observations of such incidents off the U.S. East Coast have been reported.[23] When the incorrect vertical distribution was used, the results were similar to those for weakly-absorbing aerosols in Figure 11, but with the curves moved vertically by $\sim 1.5\%$ (Figure 11a), $\sim 1.7\%$ (Figure 11b), and $\sim 2\%$ (Figure 11c), i.e., the error for $\theta_0 = 45°$ near $\theta_T = 0$ was $\sim 3.7\%$ for the U50 aerosol compared to $\sim 1.7\%$ for T50 (Figure 11c). When the correct vertical structure in τ_a was used, and the aerosol was assumed to have the same $\omega_0 P(\Theta)$ in both layers in the retrieval and prediction codes, the results were significantly improved. In this case, the curves were similar to those in Figure 12, having the values of $\sim 1\%$, $\sim 1.3\%$, and $\sim 2\%$ near $\theta_T = 0$ for $\theta_0 = 60°$, 50°, and 45°, respectively. Clearly, replacing the weakly-absorbing T50 with the strongly-absorbing U50 increases the overall error in ρ_T; however, the error can be reduced significantly by knowing the correct vertical structure.

5.C. Use of a flat sea surface in the inversion algorithm.

In all of the simulations discussed thus far it has been assumed that the sea surface was flat, i.e., there were no surface waves; however, even under light wind conditions the surface will become roughened. To understand the effect of ignoring the surface roughness in the retrieval code, we simulated the surface and TOA radiances for an ocean obeying the Cox and Munk[24] surface slope

distribution with a wind speed of $\sim$ 7.5 m/s. The simulated radiances were then used in the retrieval code, which employs a flat sea surface, to estimate $\omega_0 P(\Theta)$. The correct value of τ_a was used and $\Theta_{\text{Min}} = 0.92°$. The retrieved $\omega_0 P(\Theta)$ was then used in the TOA-radiance prediction code, which included the correct surface roughness, to estimate the TOA radiance. Thus, the assumption of a flat sea surface was used *only* in the retrieval code. The resulting error in the TOA radiance is presented in Figure 13, which shows that the error using this procedure is similar to that when the surface is actually flat (Figure 6) except near $\theta_T \approx 37°$ for $\theta_0 = 50°$ and $\theta_T \approx 45°$ for $\theta_0 = 45°$ (Figures 6c and 6d). The dissimilarity at these values of θ_T is due to the absence of the "spike" in the retrieved $\omega_0 P(\Theta)$ near $\Theta = 120°$ in the rough surface case. Recall, the spike was due to backscattering following reflection of direct solar radiation from the surface. When the surface is rough, the reflected solar beam is diffused over a range of angles, so ρ_B does not contain a maximum opposite the reflected solar beam. Rather, the radiance backscattered from the reflected solar beam is spread over a range of θ_B and the error it induces in the retrieved $\omega_0 P(\Theta)$ is no longer concentrated near $\Theta = 120°$. Note that the correct surface roughness was used in the prediction code for ρ_T. This is acceptable, as surface measurements of the wind speed would be expected to be available at any ρ_B-measurement site, i.e., the correct value of the wind speed could always be used with the flat-surface retrieved $\omega_0 P(\Theta)$ to estimate the TOA radiance.

5.D. Approximation of a plane-parallel atmosphere in the inversion algorithm.

Thus far, we have been assuming that radiative transfer in the atmosphere could be adequately approximated by treating the atmosphere as a plane-parallel medium (PPM), i.e., we have ignored the curvature of the atmosphere. To understand the error in our procedure induced by this assumption, we used a two-layer Monte Carlo radiative transfer code in spherical geometry[25] to simulate the normalized radiance that would be measured at the top and bottom of an atmosphere, ρ_T and ρ_B, modeled as a spherical shell medium (SSM). In the code it was assumed that the aerosol layer was 2 km thick and the molecular-scattering layer was 18 km thick (the total thickness of the atmosphere was 20 km). The aerosol optical properties were provided by the M99 model (Figure 2). The values of ρ_B in the solar almucantar and principal plane from this code were then inserted in the retrieval program (that assumes the atmosphere is plane parallel) and $\omega_0 P(\Theta)$ was retrieved.

The retrieved $\omega_0 P(\Theta)$ was then used in the plane-parallel prediction code to compute the radiance at the top of the atmosphere for comparison with ρ_T. Figure 14 provides the comparison between the predicted and true values of ρ_T using this procedure. This figure should be compared with Figure 6, which used the identical procedure except that the "true" values of ρ_T and ρ_B were also generated for a plane-parallel atmosphere. Other than the ragged nature of the curves in Figure 14 (caused by Monte Carlo fluctuations in both the ρ_B pseudo data used in the retrieval algorithm and in ρ_T used to test the efficacy of the procedure), there is no significant difference between the two simulations. This suggests that the approximation of a plane-parallel atmosphere does not significantly degrade the prediction ρ_T, for $\theta_0 \sim 60°$.

5.E. Ignoring polarization in the inversion algorithm.

In our simulations, scalar radiative transfer theory (ignores polarization) has been used in all of the inversions. However, it is known that scalar theory leads to error in the computed radiance of a few percent.[26,27] To understand the error that could result from the use of scalar theory, we used vector theory (includes polarization) to create the sky radiance pseudo data ρ_B and the "true" TOA radiance ρ_T. The scattering phase matrix used in the simulation was computed from the aerosol model (M99) size distribution and index of refraction using Mie theory. The resulting values of ρ_B were then inserted into the inversion algorithm (scalar) and the phase function and single scattering albedo were retrieved. These were then used in the scalar radiative transfer equation to compute the TOA radiance. The results are provided in Figure 15 for $\theta_0 = 60°$ with $\Theta_{\min} = 0.92°$ and 2.62°. To see the effect of ignoring polarization, compare Figures 15a and 15b with Figures 6b and 8a, respectively. We note that when polarization is included in the pseudo data, but neglected in the inversion algorithm and the prediction code, there is little difference in the retrieval error near $\theta_T = 0$, however, the difference gradually increases to become about 2% near $\theta_T = 40°$. The error in the predicted TOA radiance ranges from $\sim +1\%$ near $\theta_T = 10°$ to $\sim -2\%$ near $\theta_T = 40°$. This error is primarily derived from two single-scattering processes: Fresnel reflection of the solar beam from the sea surface and subsequent aerosol scattering toward the sensor; and aerosol scattering toward the sea surface and subsequent Fresnel reflection from the sea surface toward the sensor. These processes lead to different values of ρ_T in scalar and vector radiative transfer theory. In

the standard Stokes vector (I,Q,U,V) representation of partially polarized light, e.g., see van de Hulst,[28] correctly accounting for these processes requires an estimate for $\Theta \lesssim 90°$ of the scattering phase matrix element that couples I and Q. This, in turn, requires measurement of the polarization (Stokes vector) associated with ρ_B.

6. Application to shorter wavelengths.

The preceeding analysis has centered on 865 nm, where the water-leaving radiance can be taken to be zero in nearly all oceanic environments, and therefore need not be measured. At shorter wavelengths, e.g., in the blue, the water-leaving reflectance transmitted to the top of the atmosphere can make a significant contribution to ρ_T, so to attempt such analysis in the blue, one must have measurements of the water-leaving reflectance. In the presence of such measurements, can the prediction of ρ_T be carried out at the accuracy suggested in Sections 4 and 5 for 865 nm? Considering the fact that the major contributor to ρ_T is molecular scattering, the properties of which are precisely known, it seems reasonable to expect that ρ_T could be estimated with even higher accuracy in the blue than in the near infrared. However, the presence of radiometric calibration errors will make a more severe impact on the retrieval algorithm in the blue because the reflectance error will be much larger in relation to the magnitude of the aerosol reflectance than it was at 865 nm. Thus, the retrieved aerosol phase function in the blue can be expected to be much poorer in the presence of similar radiometric calibration errors than at 865 nm. In this section we examine the accuracy that one might realistically expect in the blue, given measurements of the water-leaving reflectance.

As in the earlier examples, we assumed the aerosol was that provided by the Shettle and Fenn[17] Maritime model for relative humidity 99%, but at a wavelength of 443 nm. The aerosol optical thickness at 443 nm was taken to be 0.20, which is approximately the value that would be obtained at 443 nm for M99 if τ_a at 865 nm were 0.20 as in the earlier sections. As before, we perform the $\omega_0 P(\Theta)$ retrievals assuming several values of τ_a (0.16, 0.18, 0.20, 0.22, and 0.24) around the correct value to simulate error in the measured value. Figures 16 and 17 provide the error in the predicted TOA radiance for various values of τ_a for $\Theta_{\mathrm{Min}} = 0.92°$ and 2.62°, respectively. We note that

the error in the predicted radiance is negligible for $\Theta_{\text{Min}} = 0.92°$, and $\lesssim 1\%$ for $\Theta_{\text{Min}} = 2.62°$, when the correct value of τ_a is used. Also, as in the case of the near infrared, a given % error in τ_a results in a much smaller % error in the predicted radiance (Figures 6 and 8–10). Figure 18 provides the error in the predicted radiance that is obtained when the correct value of τ_a is used in the retrieval and prediction, but the measurement of ρ_B is assumed to have a $\pm 5\%$ error. As in the near infrared (Figure 7) the error in the predicted radiance is somewhat less than the radiometric error. These simulations suggest that, given measurements of the water-leaving radiance in the blue, the predictability of the TOA radiance from measurements made at the surface is as good at 443 nm as it is at 865 nm.

7. Concluding remarks

In this paper we have examined the accuracy that one could expect in estimating the reflectance ρ_T of the ocean-atmosphere system based on a measurement suite carried out at the sea surface. Simulations were carried out in which the aerosol scattering phase function and single scattering albedo were derived when the solar zenith angle was 60°. Based on these retrievals, ρ_T was estimated for $\theta_0 = 60°$, 50°, and 45°, under the assumption that the aerosol optical properties, as defined by $\omega_0 P(\Theta)$ do not change as θ_0 varies from 60° to 45°.

Initially, the wavelength was taken to be 865 nm, as the water-leaving radiance at this wavelength would be negligible in all but the most turbid coastal waters. Also, it was assumed that there were no errors in the measurements of the sky radiance, ρ_B, and in the aerosol optical thickness τ_a.

For viewing angles $\theta_T \lesssim 20°$ the error in the predicted radiance at the top of the atmosphere was typically $\lesssim 1\%$ when measurements of the solar aureole were made with $\Theta_{\text{Min}} = 0.92°$ (Figure 6). Omitting the solar aureole increases the error because it is then inconsistent to use the correct value of τ_a in the inversion-prediction process. However, if the correct value of ω_0 can be estimated, e.g., in the case of a locally-generated maritime aerosol for which $\omega_0 \approx 1$, excellent results can still be obtained if the value of τ_a that provides the correct value of ω_0 in the inversion algorithm is also used in the prediction algorithm. Alternatively, if a wide-field-of-view sun photometer is used to

estimate τ_a, and the sky radiance measurements exclude the portion of the solar aureole observed by the sun photometer, then using this photometer-measured value of τ_a in the inversion-prediction process will yield an excellent prediction of ρ_T (Appendix A, Figure 19).

We systematically investigated the influence of the simplifying assumptions made in the inversion-prediction process, such as, modeling the atmosphere as a plane-parallel medium, employing a smooth sea surface in the inversion algorithm, using scalar radiative transfer theory, and assuming that the aerosol was confined to a thin layer just above the sea surface. In most cases, these assumptions did not increase the error beyond $\pm 1\%$. The single exception was the use of scalar radiative transfer theory, for which the error grew to as much as $\sim 2\%$ for $\theta_T \gtrsim 30°$, even though it was within $\pm 1\%$ for $\theta_T \lesssim 20°$ (Figure 15). This error could be reduced by measuring the polarization associated with ρ_B, and using an inversion-prediction code that includes polarization.

In simulations in which the aerosol consisted of two types (M99 uniformly mixed in the marine boundary layer and T50 uniformly mixed in the free troposphere), knowledge and use of the vertical distribution of τ_a, as might be inferred from LIDAR measurements, did not appreciably improve the predicted ρ_T over that predicted by assuming all of the aerosol was in the marine boundary layer. This suggests that the vertical distribution of the aerosol is unimportant; however, this derives from the fact that the aerosol models used were only weakly absorbing. When T50 was replaced by the strongly-absorbing U50, sensitivity to the vertical structure was observed. Also, the error was larger than that for the weakly-absorbing aerosols, suggesting that, for the purpose of vicarious calibration of space-borne radiometers, regions that may be influenced by strongly-absorbing aerosols should be avoided.

It is possible to extend this analysis to the blue region of the spectrum, when ρ_w is available there. We found significantly better predictions of ρ_T in the blue (443 nm) than in the NIR because a major portion of ρ_T is the result of molecular scattering, which is precisely known.

It is important to note that our simulations have been carried out using the Shettle and Fenn[17] M99 phase function (Figure 2), which has a very sharp forward peak. As the $\omega_0 P(\Theta)$ retrieval algorithm performs most poorly with such phase functions, we believe that the results

described in this paper represent a near worst-case scenario. In general, the error in the retrieved $\omega_0 P(\Theta)$ and the predicted ρ_T should be significantly less than that provided by M99.

We also simulated the influence of calibration errors in both the sun photometer and the ρ_B radiometer. The results suggest that the relative error in the predicted ρ_T is similar in magnitude to that in the measured ρ_B (actually it is somewhat less). However, the relative error in ρ_T induced by error in τ_a is usually $\ll$ the relative error in τ_a (Figure 6), and in fact, as τ_a becomes small (single scattering) error in τ_a becomes irrelevant (Eq. (4)).

The purpose of undertaking this study was to investigate the accuracy that one might reasonably expect in computing the TOA radiance for the purpose of vicarious calibration of space-borne sensors. We note the results presented here apply only to the idealized case of a cloud-free sky and a horizontally-homogeneous aerosol. However, we do not consider this a blemish. We believe a reasonable strategy for vicarious calibration over the oceans in the NIR ($\rho_w = 0$) is to place unattended sun photometer/sky radiometer units[29] on small remote islands, but to use, for vicarious calibration, only the surface data that was acquired simultaneously with ρ_T under near-ideal conditions. Under such circumstances, the results presented here should be applicable.

It is now possible to calibrate a radiometer relative to a standard lamp to within $\pm 2.5\%$,[12] although it is believed that detector-based calibration could reduce the uncertainty to $\pm 1\%$.[30] Thus, from our simulations, it appears safe to conclude that at present, the most important error source in the prediction of ρ_T from ρ_B is likely to be error in the ρ_B measurement.

Appendix A: Is the solar aureole really needed?

It is interesting to see if there is a method of dealing with the absence of the solar aureole without having to resort to assuming the $\omega_0 = 1$ for the aerosol as described in the text. Here we examine the possibility of using a wide-field-of-view sun photometer to measure the appropriate optical thickness to be used in the retrieval. The idea is simple: if sky radiance measurements can only be made at angles greater than α from the sun, use a sun photometer that has an acceptance half angle of α. In this way, neglecting multiple scattering near the aureole, the photometer will measure an optical thickness $\tau_a^{(m)}$ that is related to the actual optical thickness τ_a through

$$\frac{\tau_a^{(m)}}{\tau_a} = \frac{\int_\alpha^\pi P(\Theta)\sin\Theta\, d\Theta}{\int_0^\pi P(\Theta)\sin\Theta\, d\Theta}.$$

$\tau_a^{(m)}$ is hypothesized to be the appropriate value of aerosol optical thickness to be used in the aureole-free retrievals, with $P(\Theta)$ truncated at $\Theta = \alpha$. Results of tests of this idea are presented in Figure 19, which provides the error in the TOA radiance when the both the inversion algorithm and the TOA-radiance prediction are carried out using $\tau_a^{(m)}$ for the four values of $\Theta_{\rm Min} = \alpha$ used in this study. For $\Theta < \Theta_{\rm Min}$, $P(\Theta)$ was taken to be $P(\Theta_{\rm Min})$ in *both* the inversion and prediction codes. For the range of θ_T of interest here ($\theta_T < 60°$) the difference between $\Theta_{\rm Min} = 0.92°$ and 17.33° is less than 1% in the error in the predicted TOA radiance and the difference between 0.92° and 8.68° is usually less than 0.4%. These results suggest that if a calibrated solar photometer were available with the proper (wide) field of view, measurement of the solar aureole would not be necessary.

References

[1] H. R. Gordon, "A preliminary assessment of the Nimbus-7 CZCS atmospheric correction algorithm in a horizontally inhomogeneous atmosphere," in *Oceanography from Space*, edited by J. R. F. Gower (Plenum Press, New York, NY, 1981) p. 257–266.

[2] H. R. Gordon, "Reduction of error introduced in the processing of coastal zone color scanner-type imagery resulting from sensor calibration and solar irradiance uncertainty," Applied Optics **20**, 207–210 (1981).

[3] P. Koepke, "Vicarious Satellite Calibration in the Solar Spectral Range by Means of Calculated Radiances and its Application to Meteosat," Applied Optics **21**, 2845–2854 (1982).

[4] M. Viollier, "Radiance calibration of the Coastal Zone Color Scanner: a proposed adjustment," Applied Optics **21**, 1142–1145 (1982).

[5] H. R. Gordon, D. K. Clark, J. W. Brown, O. B. Brown, R. H. Evans and W. W. Broenkow, "Phytoplankton pigment concentrations in the Middle Atlantic Bight: comparison between ship determinations and Coastal Zone Color Scanner estimates," Applied Optics **22**, 20–36 (1983).

[6] H. R. Gordon, J. W. Brown, O. B. Brown, R. H. Evans and D. K. Clark, "Nimbus 7 Coastal Zone Color Scanner: reduction of its radiometric sensitivity with time," Applied Optics **22**, 3929–3931 (1983).

[7] W. A. Hovis, J. S. Knoll and G. R. Smith, "Aircraft Measurements for Calibration of an Orbiting Spacecraft Sensor," Applied Optics **24**, 407–410 (1985).

[8] R. S. Fraser and Y. J. Kaufman, "Calibration of satellite sensors after launch," Applied Optics **25**, 1177–1185 (1986).

[9] P. N. Slater, S. F. Biggar, R. G. Holm, R. D. Jackson, Y. Mao, M. S. Moran, J. M. Palmer and B. Yuan, "Reflectance- and Radiance-Based Methods for the In-Flight Absolute Calibration of Multispectral Sensors," Remote Sensing of Environment **22**, 11–37 (1987).

[10] R. Frouin and C. Gautier, "Calibration of NOAA-7 AVHRR, GOES-5, and GOES-6 VISSR/VAS Solar Channels," Remote Sensing of Environment **22**, 73–101 (1987).

[11] Y. J. Kaufman and B. N. Holben, "Calibration of the AVHRR visible and near-IR bands by atmospheric scattering, ocean glint, and desert reflection," Int. Jour. Rem. Sens. **14**, 21–52 (1993).

[12] S. F. Biggar, P. N. Slater and D. I. Gellman, "Uncertainties in the in-flight calibration of sensors with reference to measured ground sites in the 0.4 to 1.1 μm range," Remote Sensing of Environment **48**, 245–252 (1994).

[13] P. Y. Deschamps, F. M. Bréon, M. Leroy, A. Podaire, A. Bricaud, J. C. Buriez and G. Sèze, "The POLDER Mission: Instrument characteristics and scientific objectives," IEEE Trans. Geoscience and Remote Sensing **32**, 598–615 (1994).

[14] S. B. Hooker, W. E. Esaias, G. C. Feldman, W. W. Gregg and C. R. McClain, *SeaWiFS Technical Report Series: Volume 1, An Overview of SeaWiFS and Ocean Color* (NASA, Greenbelt, MD, Technical Memorandum 104566, July 1992).

[15] V. V. Salomonson, W. L. Barnes, P. W. Maymon, H. E. Montgomery and H. Ostrow, "MODIS: Advanced Facility Instrument for Studies of the Earth as a System," IEEE Geosci. Rem. Sens. **27**, 145–152 (1989).

[16] M. Wang and H. R. Gordon, "Retrieval of the Columnar Aerosol Phase Function and Single Scattering Albedo from Sky Radiance over the Ocean: Simulations," Applied Optics **32**, 4598–4609 (1993).

[17] E. P. Shettle and R. W. Fenn, *Models for the Aerosols of the Lower Atmosphere and the Effects of Humidity Variations on Their Optical Properties* (Air Force Geophysics Laboratory, Hanscomb AFB, MA 01731, AFGL–TR–79-0214, 1979).

[18] P. J. Reddy, F. W. Kreiner, J. J. Deluisi and Y. Kim, "Aerosol Optical Depths Over the Atlantic Derived From Shipboard Sunphotometer Observations During the 1988 Global Change Expedition," Global Biogeochemical Cycles **4**, 225–240 (1990).

[19] G. K. Korotaev, S. M. Sakerin, A. M. Ignatov, L. L. Stowe and E. P. McClain, "Sun-Photometer Observations of Aerosol Optical Thickness over the North Atlantic from a Soviet Research Vessel for Validation of Satellite Measurements," Jour. Atmos. Oceanic Technol. **10**, 725–735 (1993).

[20] Y. V. Villevalde, A. V. Smirnov, N. T. O'Neill, S. P. Smyshlyaev and V. V. Yakovlev, "Measurement of Aerosol Optical Depth in the Pacific Ocean and North Atlantic," Jour. Geophys. Res. **99D**, 20983–20988 (1994).

[21] T. Nakajima, M. Tanaka and T. Yamauchi, "Retrieval of the Optical Properties of Aerosols from Aureole and Extinction Data," Applied Optics **22**, 2951–2959 (1983).

[22] K. J. Voss and G. Zibordi, "Radiometric and Geometric Calibration of a Visible Spectral Electro-Optic "Fisheye" Camera Radiance Distribution System," Jour. Atmos. and Oceanic Technology **6**, 652–662 (1989).

[23] S. Ismail, E. V. Browell, S. A. Kooi and G. D. Nowicki, "Simultaneous LASE and LITE Aerosol Profile Measurements over the Atlantic," EOS, Transactions, American Geophysical Union **76**, S71 (1995).

[24] C. Cox and W. Munk, "Measurements of the Roughness of the Sea Surface from Photographs of the Sun's Glitter," Jour. Opt. Soc. of Am. **44**, 838–850 (1954).

[25] K. Ding and H. R. Gordon, "Atmospheric correction of ocean color sensors: Effects of earth curvature," Applied Optics **33**, 7096–7016 (1994).

[26] G. W. Kattawar, G. N. Plass and S. J. Hitzfelder, "Multiple scattered radiation emerging from Rayleigh and continental haze layers. 1: Radiance, polarization, and neutral points," Applied Optics **15**, 632–647 (1976).

[27] H. R. Gordon, J. W. Brown and R. H. Evans, "Exact Rayleigh Scattering Calculations for use with the Nimbus-7 Coastal Zone Color Scanner," Applied Optics **27**, 862–871 (1988).

[28] H. C. van de Hulst, *Multiple Light Scattering* (Academic Press, New York, 1980), 739 pp.

[29] B. N. Holben, T. F. Eck, I. Slutsker, D. Tanre, J. P. Buis, A. Setzer, E. Vermote, J. Reagan, Y. Kaufman, T. Nakajima, F. Lavenu and I. Jankowiak,, 1996, Automatic Sun and Sky Scanning Raiometer System for Network Aerosol Monitoring, *Remote Sensing of Environment* (Accepted) .

[30] P. N. Slater, S. F. Biggar, K. J. Thome, D. I. Gellman and P. R. Spyak, *Journal of Atmospheric and Oceanic Technology* (1995), (In press).

Figure Captions

Figure 1. The basic idea behind vicarious calibration. BOA and TOA are, respectively, the top and bottom of the atmosphere. L_T and L_B are the radiances measured at the TOA and BOA for a solar zenith angle θ_0. In the geometry shown, the single-scattering angle Θ is common to both L_T and L_B.

Figure 2. Scattering phase functions for the Shettle and Fenn[17] Maritime aerosol models with a relative humidity of 99% (M99) and the Tropospheric model with relative humidity 50% (T50).

Figure 3. Error in the retrieved $\omega_0 P(\Theta)$ for the M99 model if the single-scattering approximation were the correct physics for radiative transfer.

Figure 4. Error in the retrieved $\omega_0 P(\Theta)$ for the M99 model when multiple scattering is included in the radiative transfer.

Figure 5. Error in the estimated ρ_T as a function of θ_T when single scattering was assumed to be the correct radiative transfer physics. The error in $\omega_0 P(\Theta)$ for this case is provided in Figure 3. There was assumed to be no contribution from molecular scattering to ρ_B or ρ_T.

Figure 6. (a): Comparison between the aerosol phase function retrieved (circles) from ρ_B at 865 nm and the true phase function (line) when $\theta_0 = 60°$ for the M99 model with $\tau_a = 0.20$ and $\Theta_{\text{Min}} = 0.92°$. (b): Error in estimation of ρ_T using the retrieved phase function in (a) with $\theta_0 = 60°$. (c): Same as (b) except $\theta_0 = 50°$. (d): Same as (c) except $\theta_0 = 45°$. In panels (b)–(d), the curves from bottom to top correspond to using $\tau_a = 0.14$, 0.16, 0.18, 0.20, 0.22, 0.24, and 0.26, in both the retrieval and prediction codes.

Figure 7. Error in ρ_T induced by a $\pm 5\%$ error in the measurement of ρ_B. The measurement of τ_a is assumed to be error-free. The retrieval of $\omega_0 P(\Theta)$ is carried out when $\theta_0 = 60°$. (a): $\theta_0 = 60°$. (b): $\theta_0 = 50°$. (c): $\theta_0 = 45°$.

Figure 8. Same as Figure 6 except $\Theta_{\text{Min}} = 2.62°$.

Figure 9. Same as Figure 6 except $\Theta_{\text{Min}} = 8.68°$.

Figure 10. Same as Figure 6 except $\Theta_{\text{Min}} = 17.33°$.

Figure 11. Error in ρ_T for a two-layer atmosphere with aerosol in both layers. The retrieval and prediction codes both assume that the aerosol is only in the lower layer and use the correct value of $\tau_a = \tau_T + \tau_B$. "R" stands for Rayleigh and "A" stands for aerosol. (a): $\theta_0 = 60°$. (b): $\theta_0 = 50°$. (c): $\theta_0 = 45°$.

Figure 12. Same as Figure 11 except the retrieval and prediction codes use the correct vertical structure in τ_a.

Figure 13. Same as Figure 6, showing the effect of sea surface roughness. Retrieval code assumes $W = 0$, while the prediction code uses the correct value of W.

Figure 14. Same as Figure 13 showing the effect of the curvature of the Earth's atmosphere. Retrieval and prediction codes assume a plane-parallel atmosphere.

Figure 15. Same as Figure 14 showing the effect of ignoring polarization in the retrieval and prediction codes: (a) $\Theta_{\text{Min}} = 0.92°$; (b) $\Theta_{\text{Min}} = 2.62°$.

Figure 16. Same as Figure 6 except the wavelength is 443 nm.

Figure 17. Same as Figure 16, except Θ_{Min} is increased from 0.92° to 2.62°.

Figure 18. Error in the predicted ρ_T at 443 nm for a $\pm 5\%$ error in ρ_B for $\Theta_{\text{Min}} = 0.92°$ (solid lines) and $\Theta_{\text{Min}} = 2.62°$ (dashed lines). Positive (negative) errors in ρ_T correspond to positive (negative) errors in ρ_B.

Figure 19. Error in the predicted ρ_T when the phase function is truncated at Θ_{Min} and the value of τ_a, measured with a sun photometer of half-angle field-of-view Θ_{Min}, is used in the retrieval

and prediction codes. τ_a = 0.187, 0.162, 0.122, and 0.92 for the curves from top to bottom, corresponding to Θ_{Min} = 0.92°, 2.62°, 8.68°, and 17.33°.

Table 1: Retrieved ω_0 for a given τ_a. True value of τ_a is 0.2 and true value of $\omega_0 = 0.998$.

τ_a:	0.14	0.16	0.18	0.20	0.22	0.24	0.26
ω_0:	1.235	1.131	1.050	0.986	0.934	0.891	0.855

Table 2: Retrieved ω_0 for a given Θ_{Min} and τ_a. The true value of τ_a is 0.20 and true value of $\omega_0 = 0.998$.

Θ_{Min}	τ_a						
	0.14	0.16	0.18	0.20	0.22	0.24	0.26
0.92°	1.235	1.131	1.050	0.986	0.934	0.891	0.855
2.62°	1.207	1.105	1.026	0.964	0.913	0.871	0.837
8.68°	1.067	0.978	0.910	0.856	0.912	0.776	0.747
17.33°	0.978	0.898	0.836	0.778	0.749	0.717	0.619

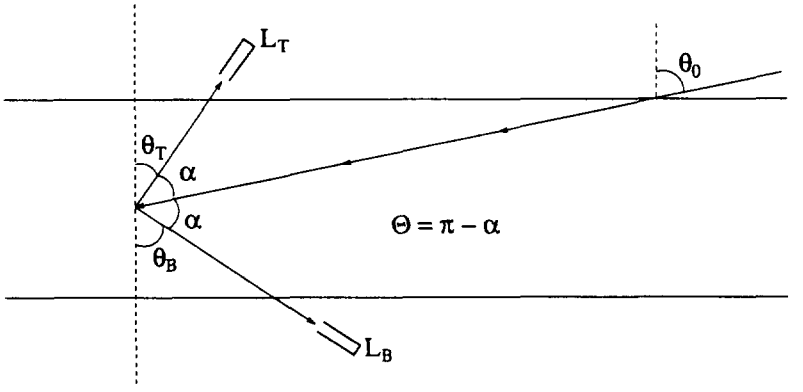

Figure 1. The basic idea behind vicarious calibration. BOA and TOA are, respectively, the top and bottom of the atmosphere. L_T and L_B are the radiances measured at the TOA and BOA for a solar zenith angle θ_0. In the geometry shown, the single-scattering angle Θ is common to both L_T and L_B.

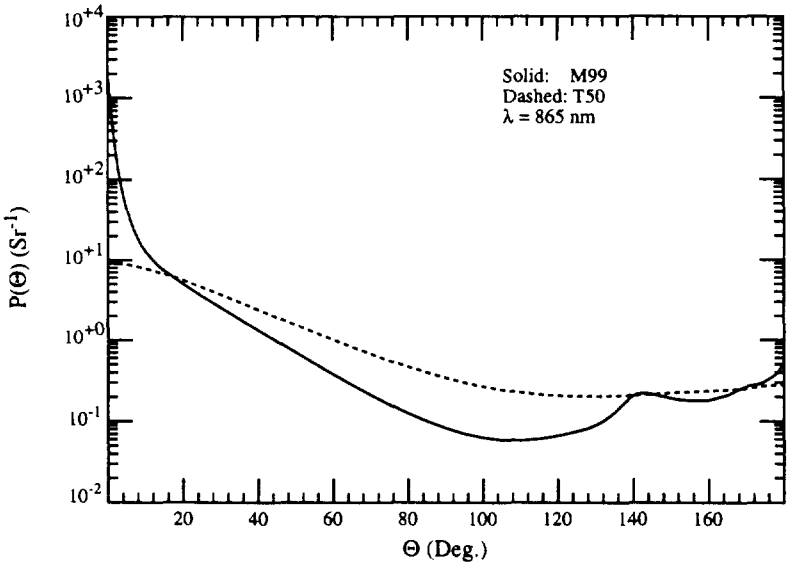

Figure 2. Scattering phase functions for the Shettle and Fenn[17] Maritime aerosol models with a relative humidity of 99% (M99) and the Tropospheric model with relative humidity 50% (T50).

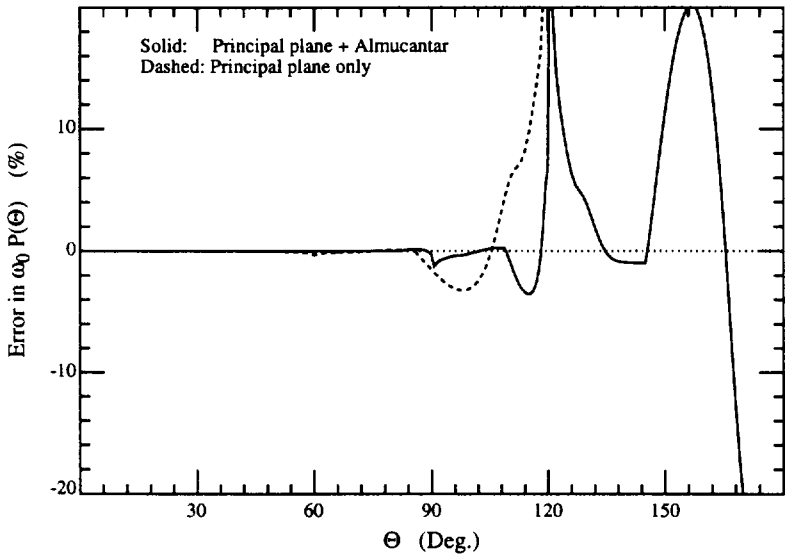

Figure 3. Error in the retrieved $\omega_0 P(\Theta)$ for the M99 model if the single-scattering approximation were the correct physics for radiative transfer.

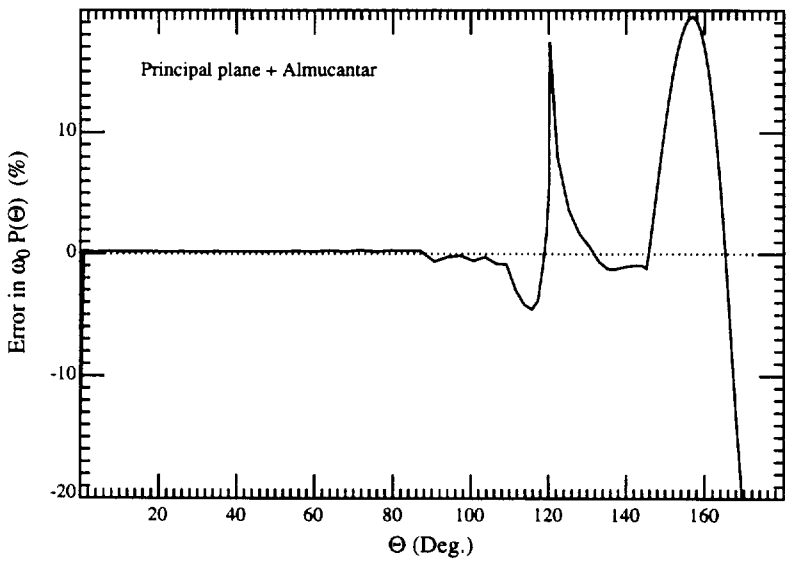

Figure 4. Error in the retrieved $\omega_0 P(\Theta)$ for the M99 model when multiple scattering is included in the radiative transfer.

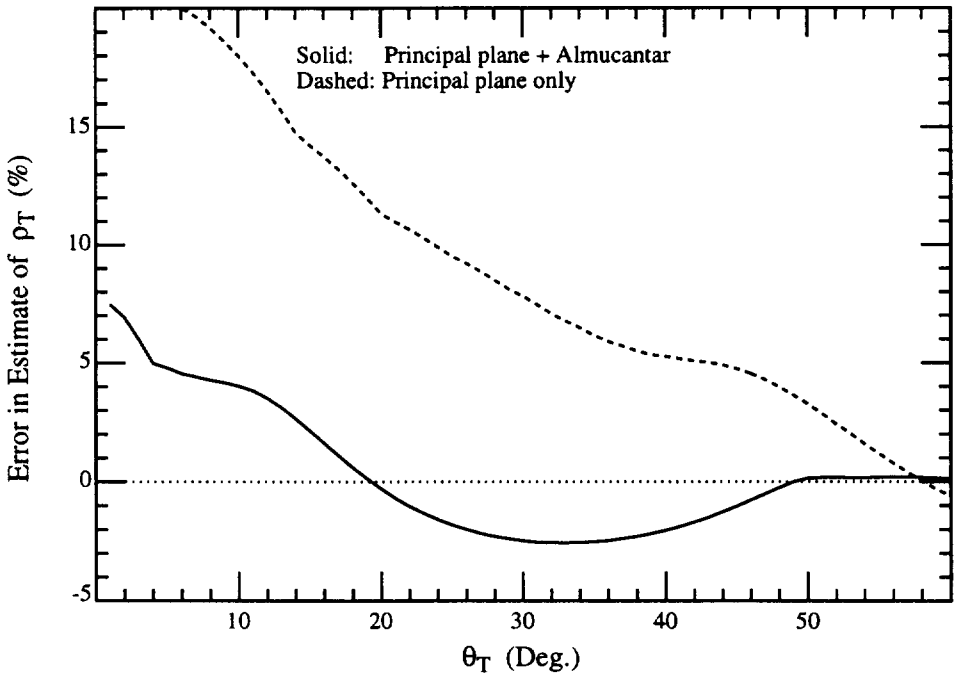

Figure 5. Error in the estimated ρ_T as a function of θ_T when single scattering was assumed to be the correct radiative transfer physics. The error in $\omega_0 P(\Theta)$ for this case is provided in Figure 3. There was assumed to be no contribution from molecular scattering to ρ_B or ρ_T.

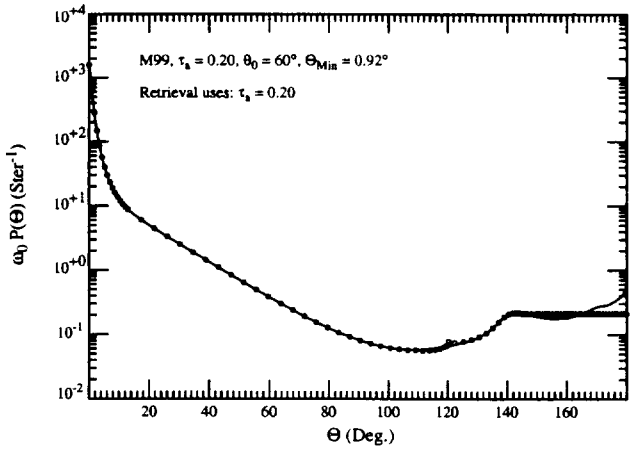

Figure 6a.

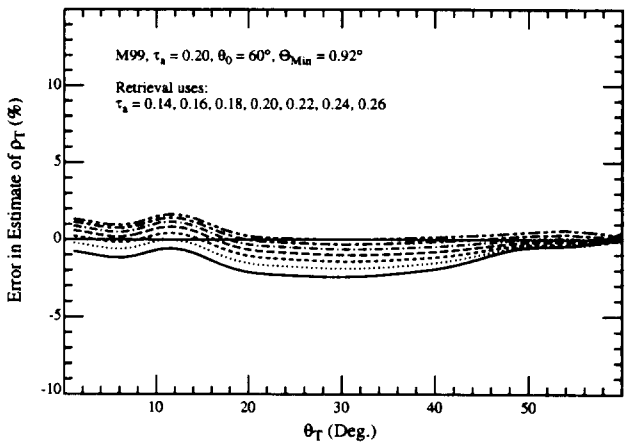

Figure 6b.

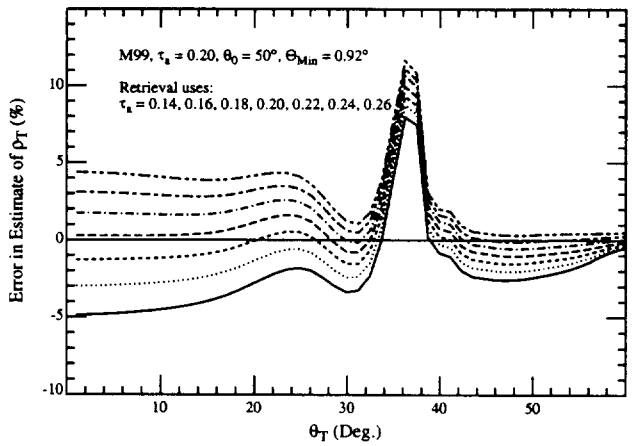

Figure 6c.

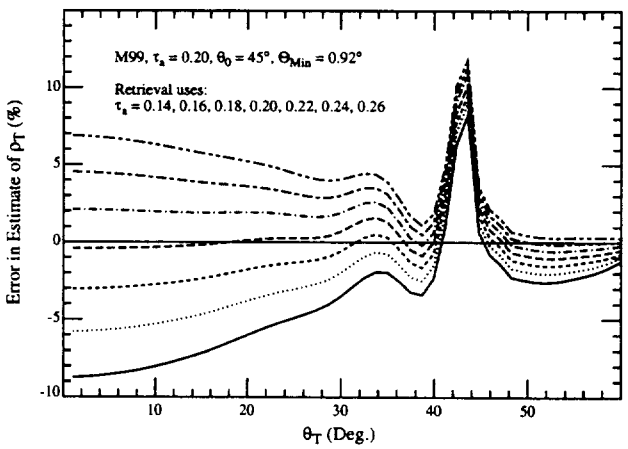

Figure 6d.

Figure 6. (a): Comparison between the aerosol phase function retrieved (circles) from ρ_B at 865 nm and the true phase function (line) when $\theta_0 = 60°$ for the M99 model with $\tau_a = 0.20$ and $\Theta_{Min} = 0.92°$. (b): Error in estimation of ρ_T using the retrieved phase function in (a) with $\theta_0 = 60°$. (c): Same as (b) except $\theta_0 = 50°$. (d): Same as (c) except $\theta_0 = 45°$. In panels (b)–(d), the curves from bottom to top correspond to using $\tau_a = 0.14$, 0.16, 0.18, 0.20, 0.22, 0.24, and 0.26, in both the retrieval and prediction codes.

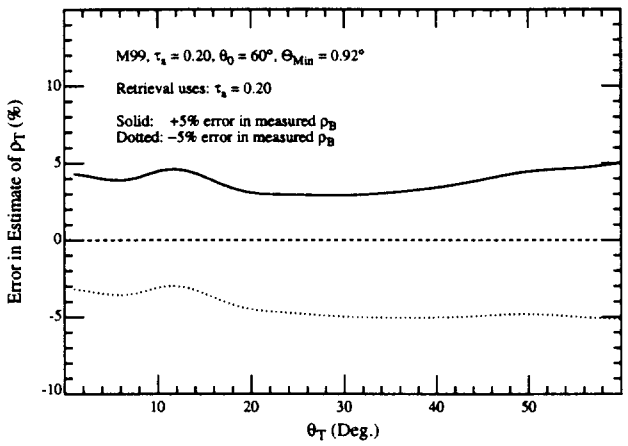

Figure 7a.

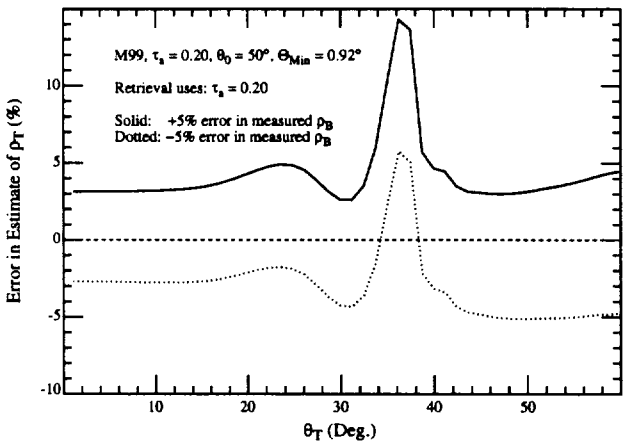

Figure 7b.

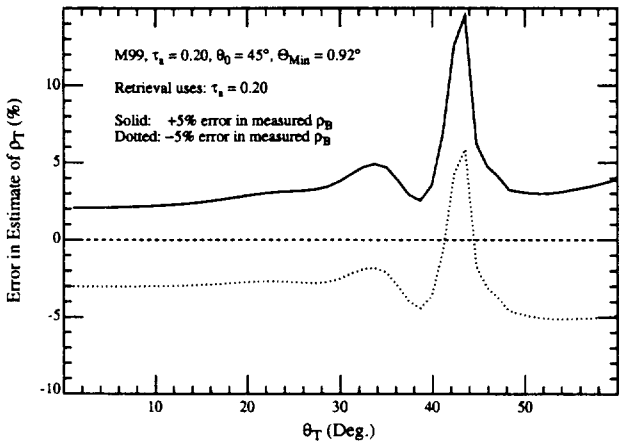

Figure 7c.

Figure 7. Error in ρ_T induced by a $\pm 5\%$ error in the measurement of ρ_B. The measurement of τ_a is assumed to be error-free. The retrieval of $\omega_0 P(\Theta)$ is carried out when $\theta_0 = 60°$. (a): $\theta_0 = 60°$. (b): $\theta_0 = 50°$. (c): $\theta_0 = 45°$.

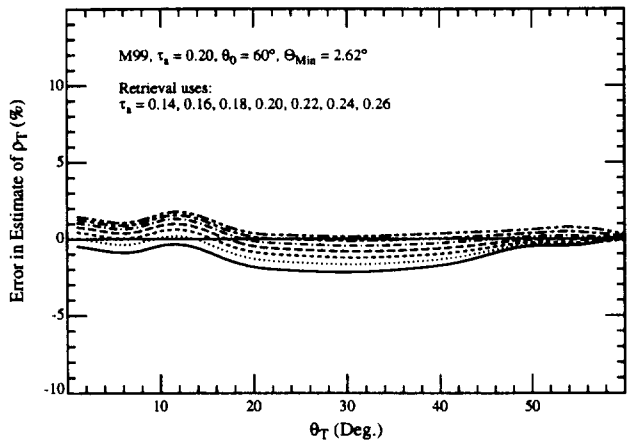

Figure 8a.

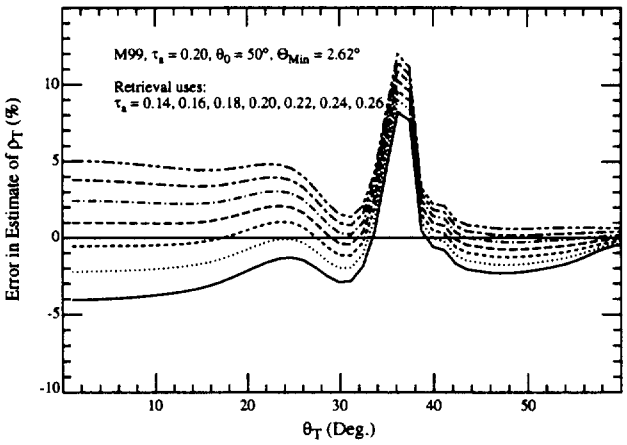

Figure 8b.

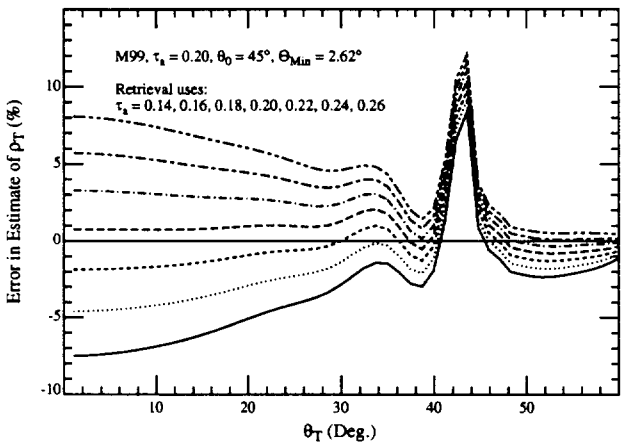

Figure 8c.

Figure 8. Same as Figure 6 except $\Theta_{Min} = 2.62°$.

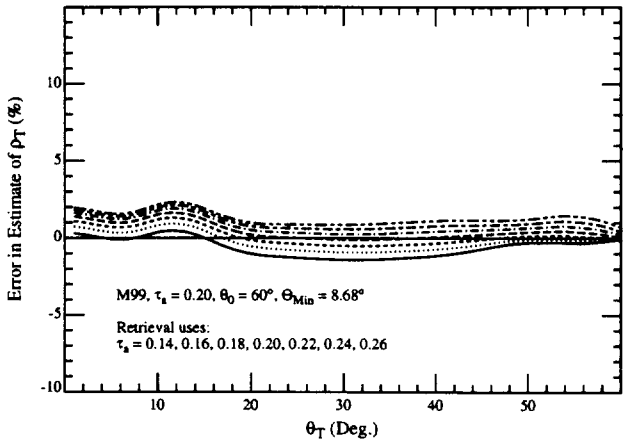

Figure 9a.

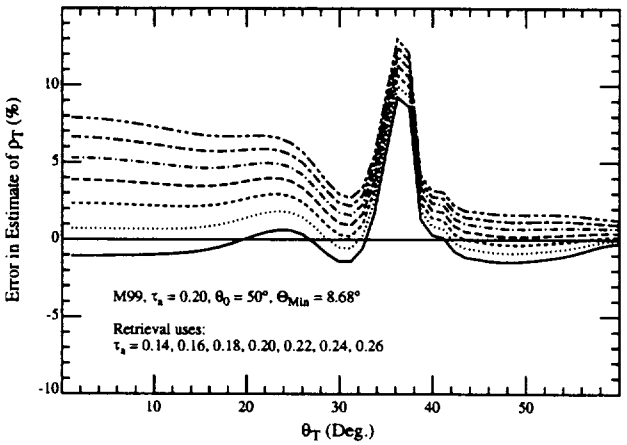

Figure 9b.

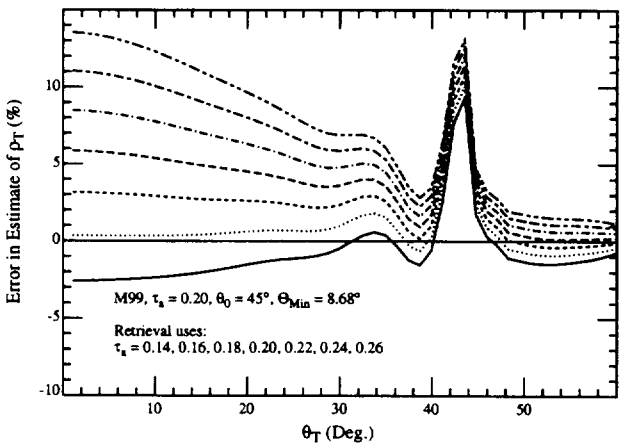

Figure 9c.

Figure 9. Same as Figure 6 except Θ_{Min} = 8.68°.

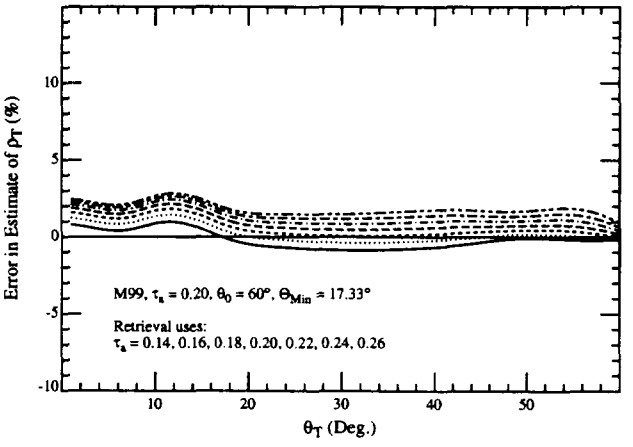

Figure 10a.

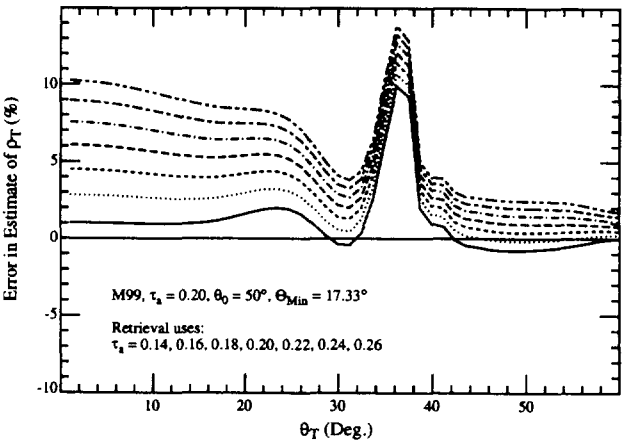

Figure 10b.

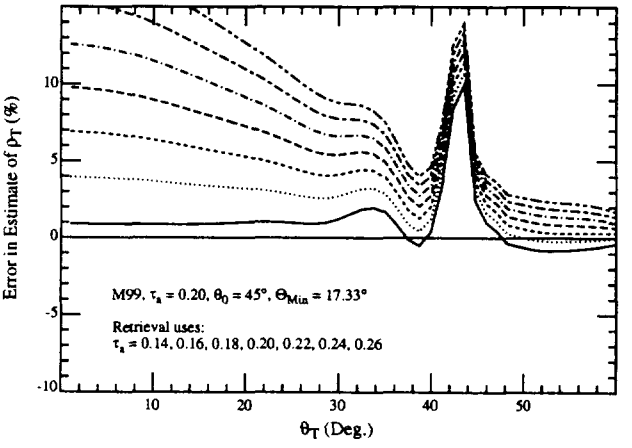

Figure 10c.

Figure 10. Same as Figure 6 except $\Theta_{Min} = 17.33°$.

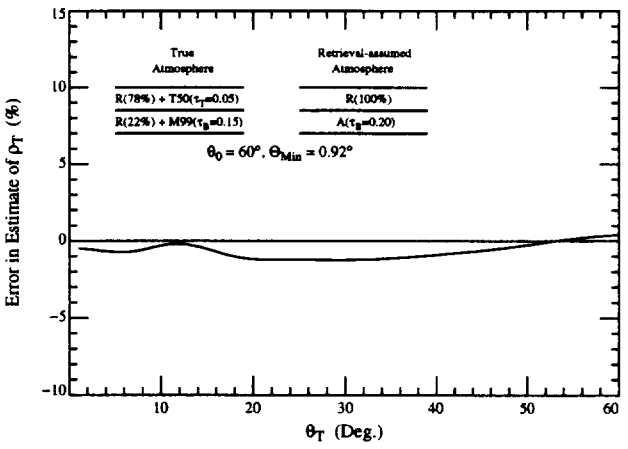

Figure 11a.

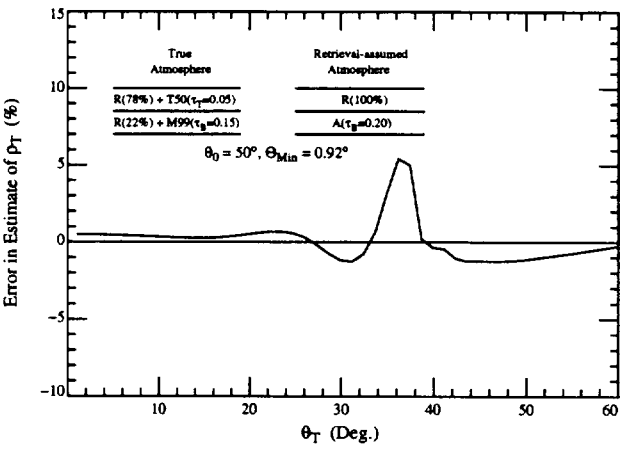

Figure 11b.

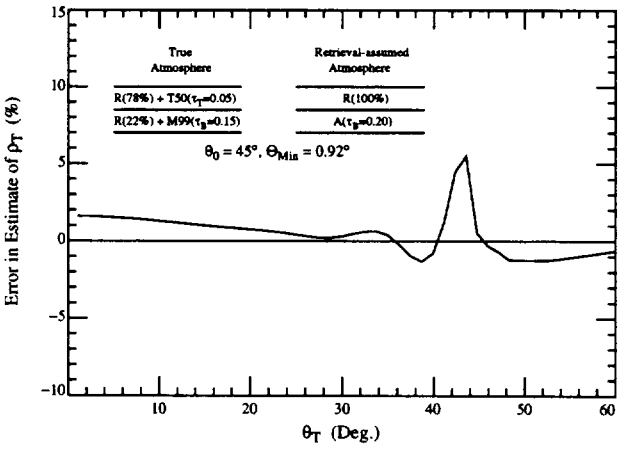

Figure 11c.

Figure 11. Error in ρ_T for a two-layer atmosphere with aerosol in both layers. The retrieval and prediction codes both assume that the aerosol is only in the lower layer and use the correct value of $\tau_a = \tau_T + \tau_B$. "R" stands for Rayleigh and "A" stands for aerosol. (a): $\theta_0 = 60°$. (b): $\theta_0 = 50°$. (c): $\theta_0 = 45°$.

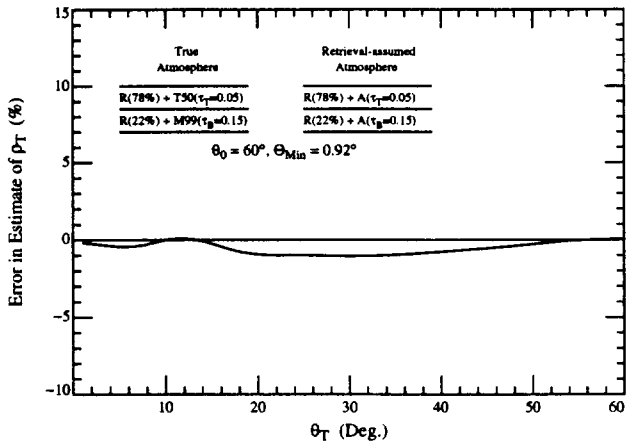

Figure 12a.

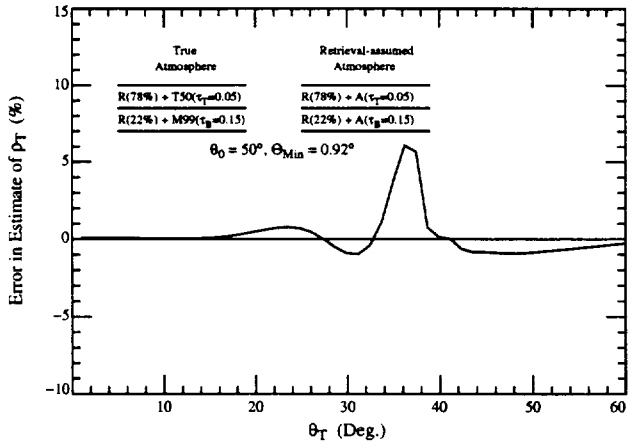

Figure 12b.

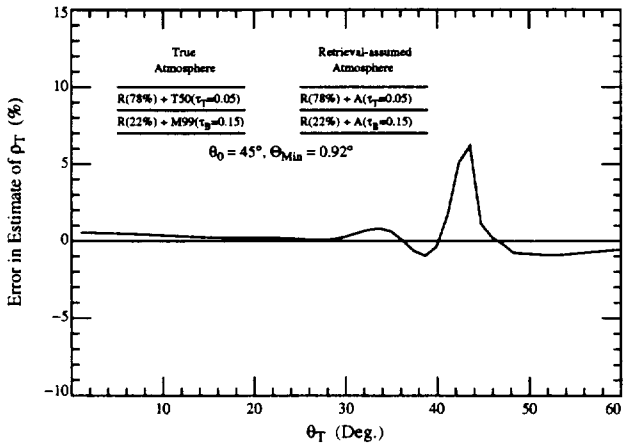

Figure 12c.

Figure 12. Same as Figure 11 except the retrieval and prediction codes use the correct vertical structure in τ_a.

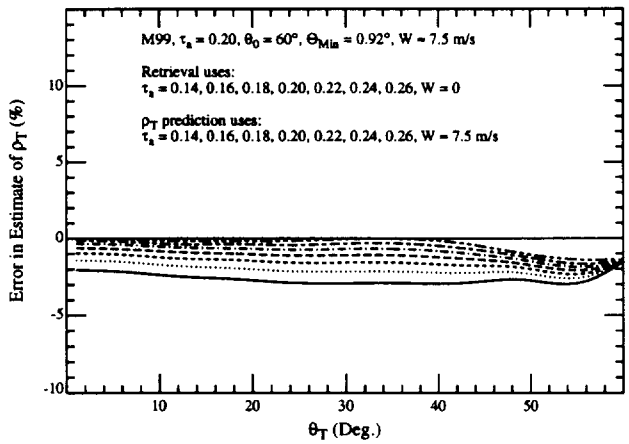

Figure 13a.

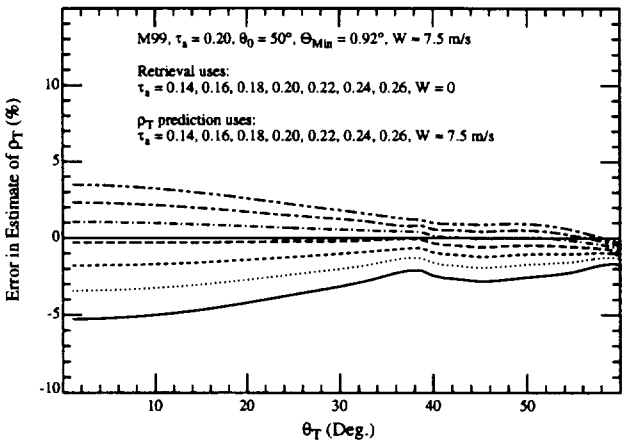

Figure 13b.

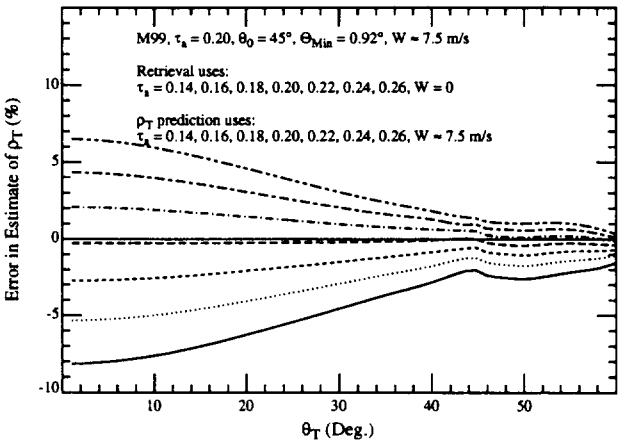

Figure 13c.

Figure 13. Same as Figure 6, showing the effect of sea surface roughness. Retrieval code assumes $W = 0$, while the prediction code uses the correct value of W.

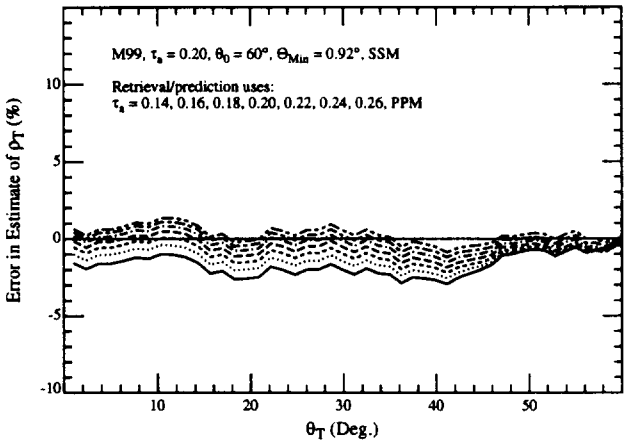

Figure 14a.

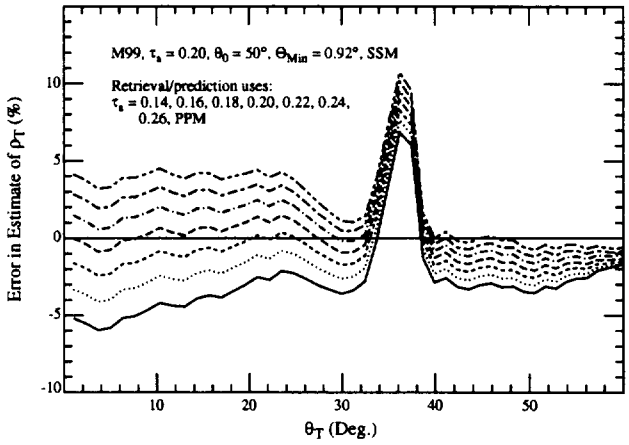

Figure 14b.

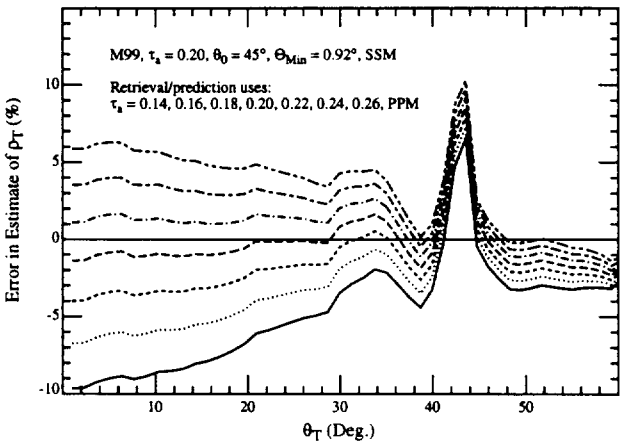

Figure 14c.

Figure 14. Same as Figure 13 showing the effect of the curvature of the Earth's atmosphere. Retrieval and prediction codes assume a plane-parallel atmosphere.

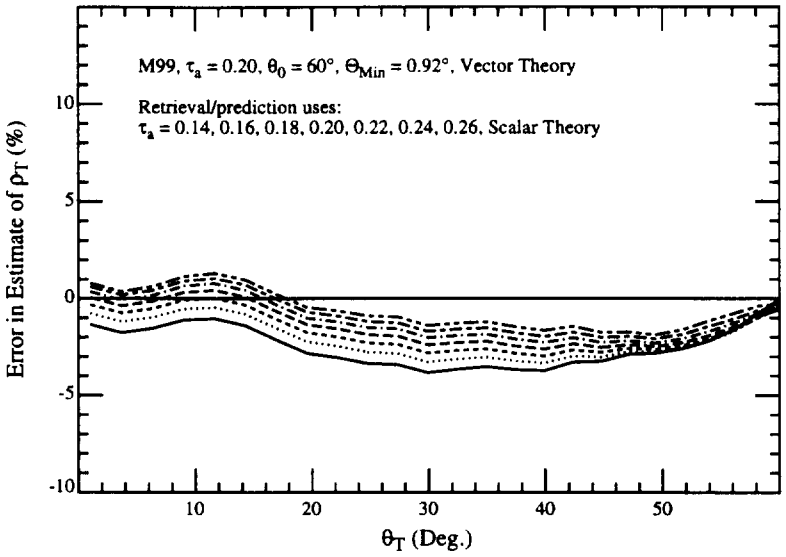

Figure 15a.

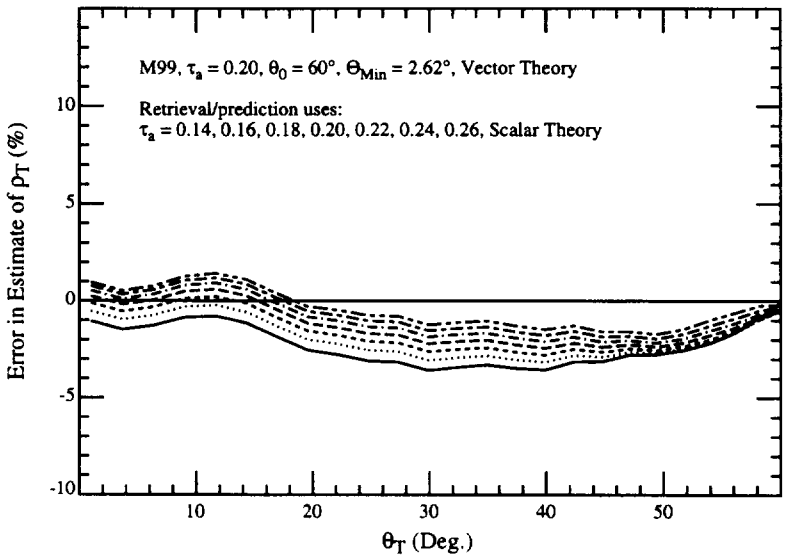

Figure 15b.

Figure 15. Same as Figure 14 showing the effect of ignoring polarization in the retrieval and prediction codes: (a) $\Theta_{Min} = 0.92°$; (b) $\Theta_{Min} = 2.62°$.

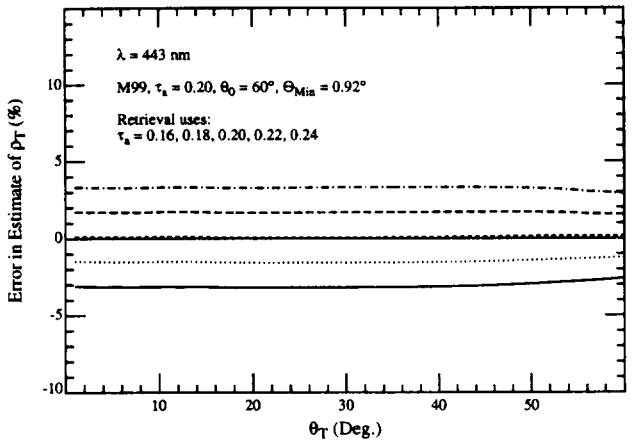

Figure 16a.

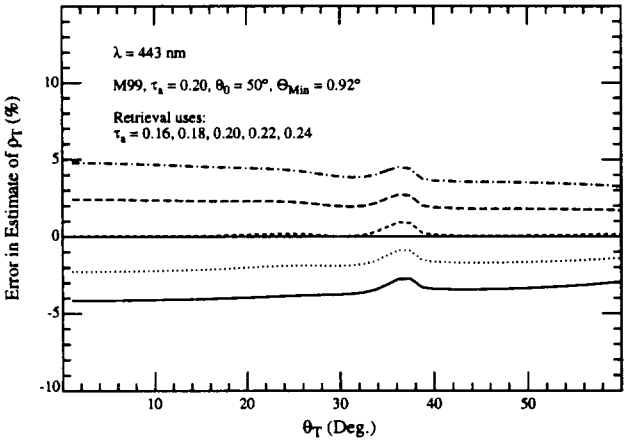

Figure 16b.

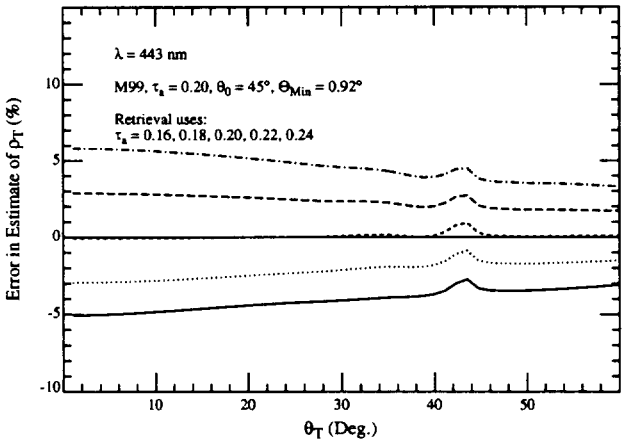

Figure 16c.

Figure 16. Same as Figure 6 except the wavelength is 443 nm.

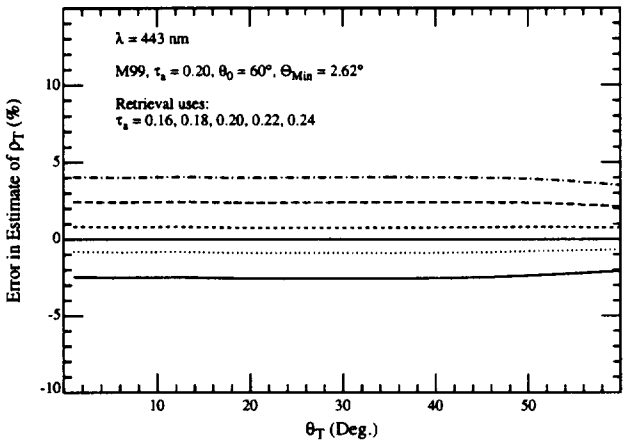

Figure 17a.

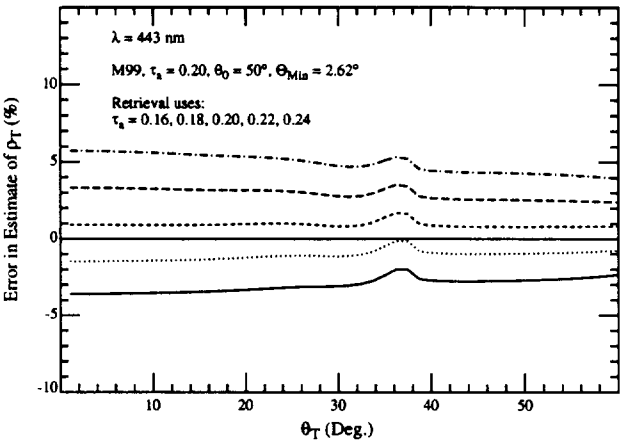

Figure 17b.

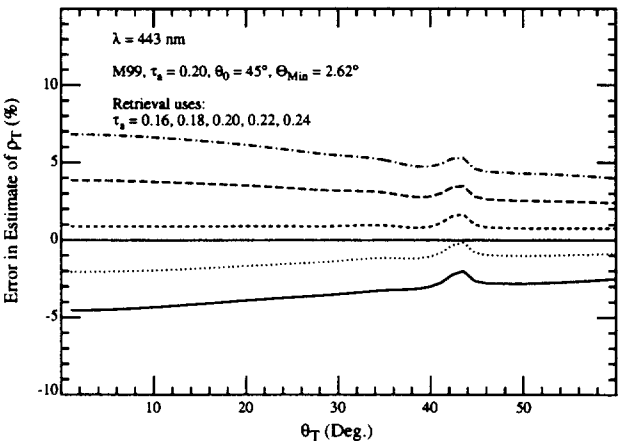

Figure 17c.

Figure 17. Same as Figure 16, except Θ_{Min} is increased from 0.92° to 2.62°.

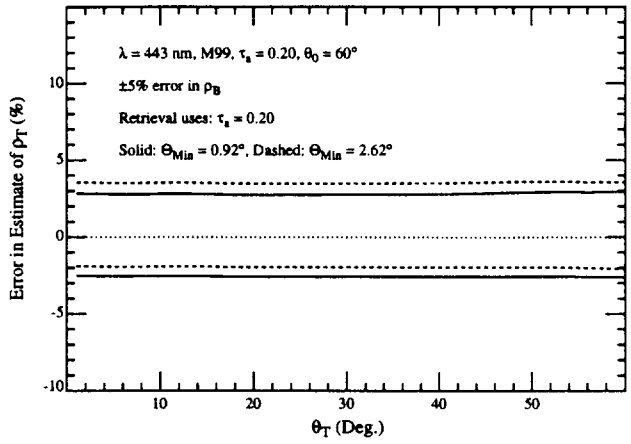

Figure 18a.

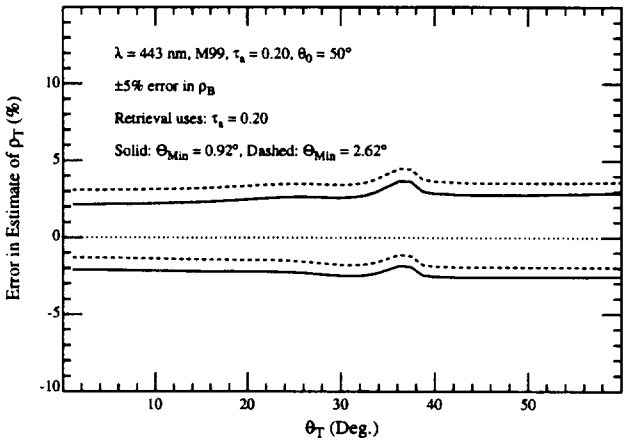

Figure 18b.

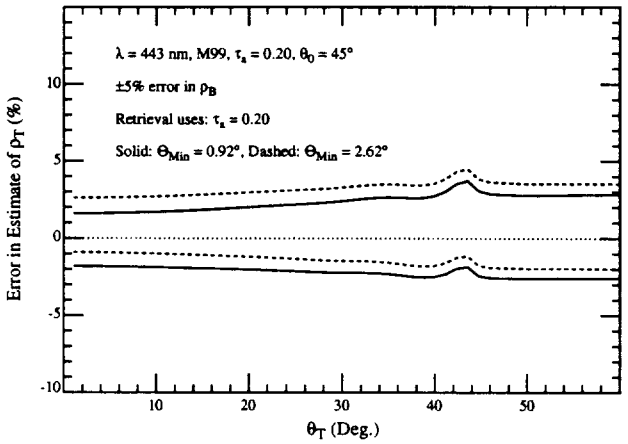

Figure 18c.

Figure 18. Error in the predicted ρ_T at 443 nm for a $\pm 5\%$ error in ρ_B for $\Theta_{\mathrm{Min}} = 0.92°$ (solid lines) and $\Theta_{\mathrm{Min}} = 2.62°$ (dashed lines). Positive (negative) errors in ρ_T correspond to positive (negative) errors in ρ_B.

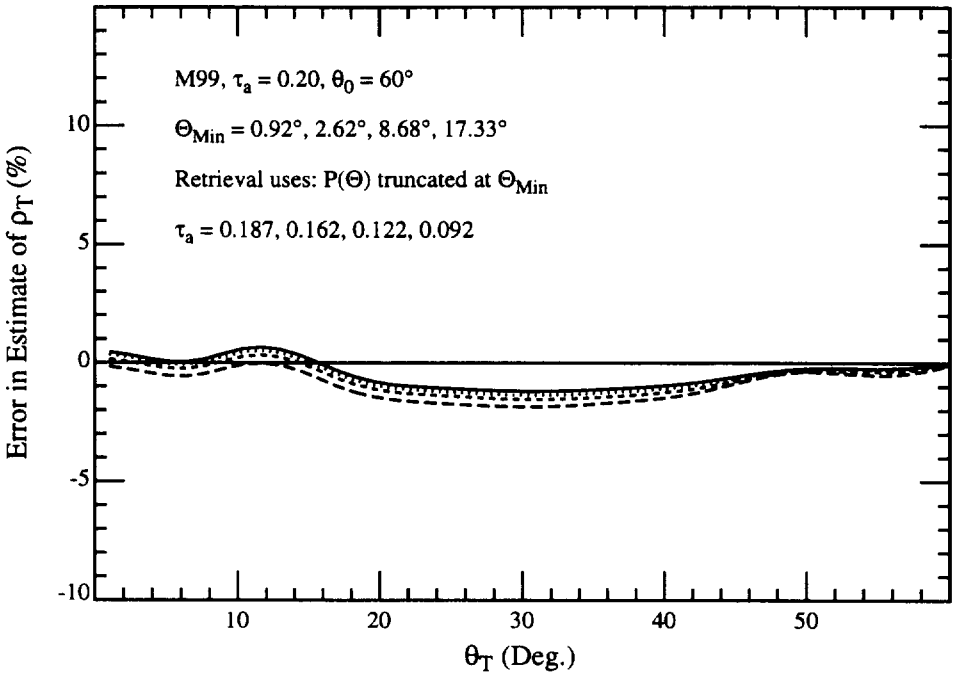

Figure 19. Error in the predicted ρ_T when the phase function is truncated at Θ_{Min} and the value of τ_a, measured with a sun photometer of half-angle field-of-view Θ_{Min}, is used in the retrieval and prediction codes. τ_a = 0.187, 0.162, 0.122, and 0.92 for the curves from top to bottom, corresponding to Θ_{Min} = 0.92°, 2.62°, 8.68°, and 17.33°.